AD-A051 845 EIKONIX CORP BURLINGTON MA F/G 14/2
HIGH RESOLUTION OPTICAL POWER SPECTRUM ANALYZER.(U)
JAN 78 N BALASUBRAMANIAN, P S CONSIDINE DAAK70-77-C-0046
UNCLASSIFIED EC/2106801-FR ETL-0127 NL

| OF |
AD
A051845

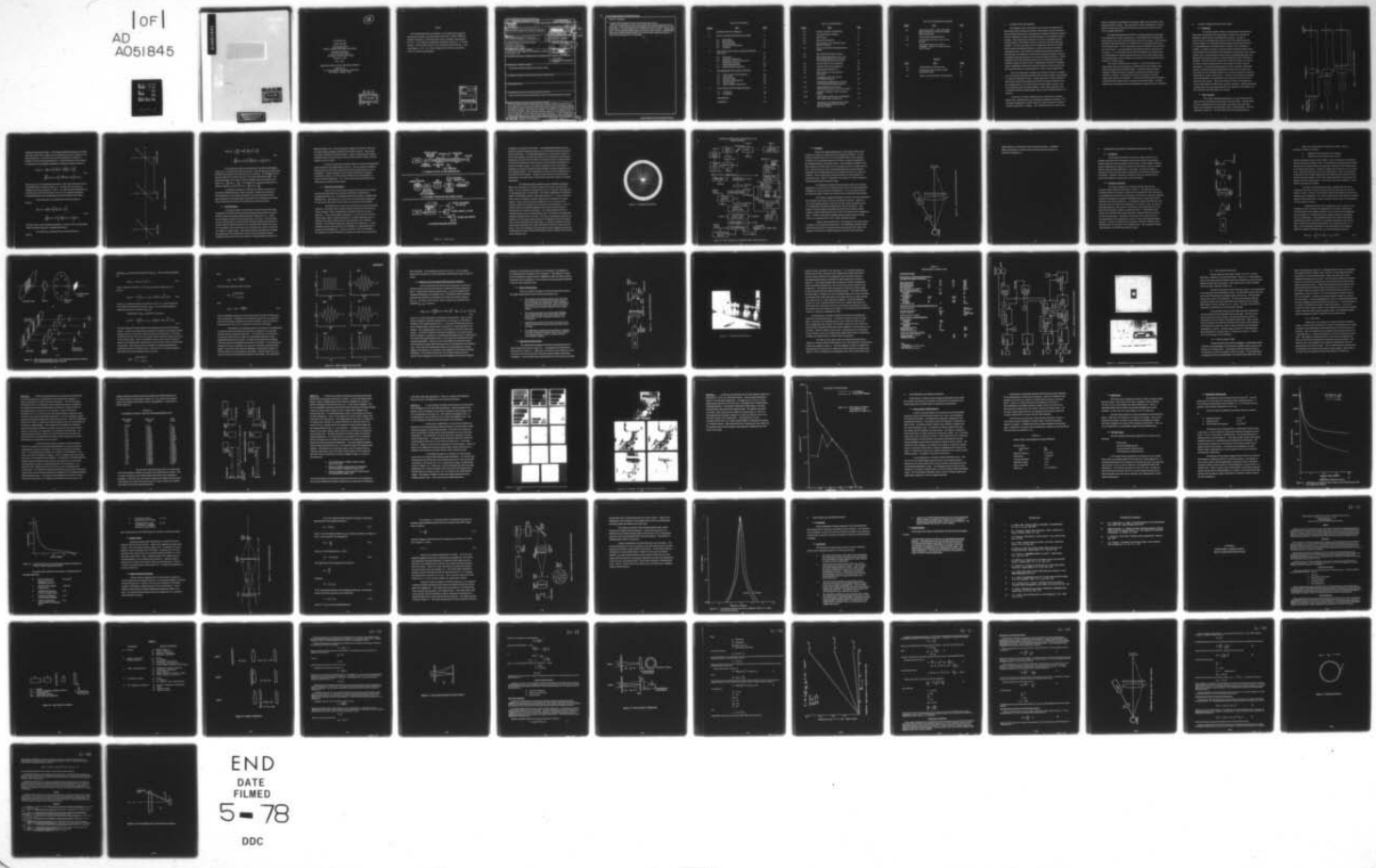

END
DATE
FILMED
5-78
DDC

(12)

EC/2106801-FR

FINAL REPORT

HIGH RESOLUTION OPTICAL POWER SPECTRUM ANALYZER

EIKONIX Corporation
103 Terrace Hall Avenue
Burlington, Massachusetts 01803

January 31, 1978

ETL - 0127

Approved for public release; distribution unlimited

Prepared for:
U. S. Army Engineer Topographic Laboratories
Fort Belvoir, Virginia 22060

Preface

This document describes an evaluation of a new optical power spectrum measurement technique, performed under Contract No. DAAK70-77-C-0046 by EIKONIX Corporation, 103 Terrace Hall Avenue, Burlington, Massachusetts for the U. S. Army Engineer Topograhpic Laboratories (USAETL), Ft. Belvoir, Virginia. The work described herein was conducted between February 2, 1977 and December 2, 1977. Dr. Robert Leighty was the USAETL Contracting Officer's Technical Representative.

SECURITY CLASSIFICATION OF THIS PAGE (When Data Entered)

REPORT DOCUMENTATION PAGE

READ INSTRUCTIONS BEFORE COMPLETING FORM

1. REPORT NUMBER: ETL-0127	2. GOVT ACCESSION NO.
3. RECIPIENT'S CATALOG NUMBER	
4. TITLE (and Subtitle): High Resolution Optical Power Spectrum Analyzer.	5. TYPE OF REPORT & PERIOD COVERED: February 2, 1977 - [redacted] Final Rept. 2 Feb - 21 Dec 77
6. PERFORMING ORG. REPORT NUMBER: EC/2106801-FR	
7. AUTHOR(s): N. Balasubramanian, P. S. Considine	8. CONTRACT OR GRANT NUMBER(s): DAAK70-77-C-0046 new
9. PERFORMING ORGANIZATION NAME AND ADDRESS: EIKONIX Corporation, 103 Terrace Hall Avenue, Burlington, Ma. 01803	10. PROGRAM ELEMENT, PROJECT, TASK AREA & WORK UNIT NUMBERS: 84p.
11. CONTROLLING OFFICE NAME AND ADDRESS: United States Army Engineering Topographic Laboratory, Fort Belvoir, Va.	12. REPORT DATE: 31 Jan [redacted] 78
	13. NUMBER OF PAGES: 83 pages
14. MONITORING AGENCY NAME & ADDRESS (if different from Controlling Office)	15. SECURITY CLASS. (of this report): Unclassified
	15a. DECLASSIFICATION/DOWNGRADING SCHEDULE

16. DISTRIBUTION STATEMENT (of this Report)

Distribution Unlimited; approved for public release

17. DISTRIBUTION STATEMENT (of the abstract entered in Block 20, if different from Report)

18. SUPPLEMENTARY NOTES

19. KEY WORDS (Continue on reverse side if necessary and identify by block number)

Optical Power Spectrum; Coherent Optics; Optical Processing; Spectral Analysis

20. ABSTRACT (Continue on reverse side if necessary and identify by block number)

The High Resolution Optical Power Spectrum Analyzer (HOPS) was conceived as a better approach to a large volume optical power spectrum (OPS) scanning of imagery. This approach enables conventional OPS measurement coupled with simplified parallel optical film sampling, rather than film scanning. The HOPS is a coherent optical system that lends itself to many applications either proposed or demonstrated, such as pattern recognition, feature extraction and image assessment. Custom configuration of HOPS enables optimum use of off-the-shelf scanning photodiode arrays and adaption

DD FORM 1 JAN 73 1473 EDITION OF 1 NOV 65 IS OBSOLETE

391 225

SECURITY CLASSIFICATION OF THIS PAGE (When Data Entered)

Block 20 Continued

to specific film scanning and spectrum sampling requirements.

This work demonstrates the basic metric equivalence between HOPS and conventional OPS. It also demonstrates the advantages of the HOPS configuration for OPS measurement. Several configurations of HOPS have been evaluated. A design using linear, self-scanned photodiode arrays with parallel optical trains is recommended. This report presents detailed analysis and measurements supporting HOPS as a highly practical approach to OPS scanning.

TABLE OF CONTENTS

LIST OF ILLUSTRATIONS

LIST OF ILLUSTRATIONS (Continued)

TABLES

1. INTRODUCTION AND SUMMARY

The mapping process in the broader sense involves the acquisition of data through remote sensing, processing of data acquired, storage and display. The processing of data involves the generation of elevation profiles and contours and the classification of natural and cultural patterns for cartographic symbol encoding. While considerable automation of the stereo compilation process has been achieved, the problem of feature extraction is still being addressed manually. In recent years there has been considerable interest in the application of optical processing techniques to achieve automation of the feature extraction process. Of the numerous techniques and concepts proposed and demonstrated, the potential use of optical power spectrum analysis for pattern recognition and image assessment has received the greatest attention. Several investigators have demonstrated already the uses of optical power spectrum analysis to simple and specific tasks of classification and pattern recognition. Custom configuration optical power spectrum analyzers are being made available commercially and are being applied to a variety of special applications.

Most of the applications of optical power spectrum analysis in mapping have to contend with large input transparencies and hence require rapid sampling of a large two-dimensional format. Current approaches to system implementation involve either the mechanical translation of the input transparency over the sampling aperture of the optical power spectrum analyzer system or the use of telecentric laser scanning techniques. Both of these approaches have considerable operational disadvantages whenever small sampling apertures are required.

In this report a system configuration for an optical power spectrum analyzer that is different from the "conventional" approach is described. The new system configuration is ideally suited for image assessment and feature extraction applications in mapping. This report documents the results of the

study to investigate the feasibility of the proposed "High resolution Optical Power Spectrum analyzer" (HOPS). The main objective of this investigation is to demonstrate the measurement concept and evaluate its performance from the point of view of mapping applications.

This report demonstrates that HOPS is a practical approach to high speed OPS measurement of image transparencies. HOPS designs with two-dimensional and one-dimensional self-scanned photodiode arrays were evaluated. HOPS measurements have been simulated and a two-dimensional se f-scanned photodiode array was set-up and tested. The two-dimensional array has limitations that prohibit its use in this system. A one-dimensional array design provides the best option for the system. It is recommended that the HOPS be configured on an optical bench for testing purposes, using one-dimensional detector arrays with parallel optics. The testing program would be designed to demonstrate the advantages and utility of HOPS for film OPS sampling.

This report is divided into five chapters. A brief introduction to the optical power spectrum measurement is presented in the second chapter along with the description of the existing systems. In the third chapter the basic principle of HOPS measurement concept is described and its unique characteristics are outlined. The differences between "conventional" and HOPS measurement data are also explained. An analysis of selected system parameters associated with the HOPS system is presented in the fourth chapter. The fifth chapter lists the conclusions and recommendations resulting from this investigation.

2. OPTICAL POWER SPECTRUM ANALYZERS

2.1 Introduction

Two decades ago the concepts of communication and information theory were introduced into the optical domain to assist in the analysis and synthesis of optical systems and photographic materials. The use of Fourier theory for analyzing optical systems lead to the realization that the Fourier transform of a coherently illuminated optical signal physically exists in a well-defined plane in an optical system and hence can be measured or modified. A number of articles on coherent optical processing provides excellent introduction to the development and applications resulting from linear systems analysis (1, 2). Of the numerous coherent optical processing applications, the application to the spectral analysis of spatial signals has received widespread attention. The basic concepts of optical power spectrum analysis are based on the Fourier transforming properties of a lens system used under coherent illumination. The analysis demonstrating the Fourier transform relationship between a coherently illuminated object placed at the front focal plane of the lens system and the amplitude distribution at its back focal plane have been well documented in a number of places (3, 4). However, for the purpose of continuity, a basic introduction to the fundamental Fourier properties of lens systems is presented in this chapter. This also provides the basis for the discussion on system configurations for optical power spectrum analyzers. Different approaches to optical power spectrum measurement are also described in this chapter, and their advantages and disadvantages are outlined.

2.2 Basic Principle

The Fourier transforming properties of a lens system forms the basis of all two-dimensional coherent optical data processing. Basically there are three configurations of the lens system with respect to the input plane object, for producing the two-dimensional Fourier transformations. They are illustrated in Figure 2-1. In each of these cases the input illumination is

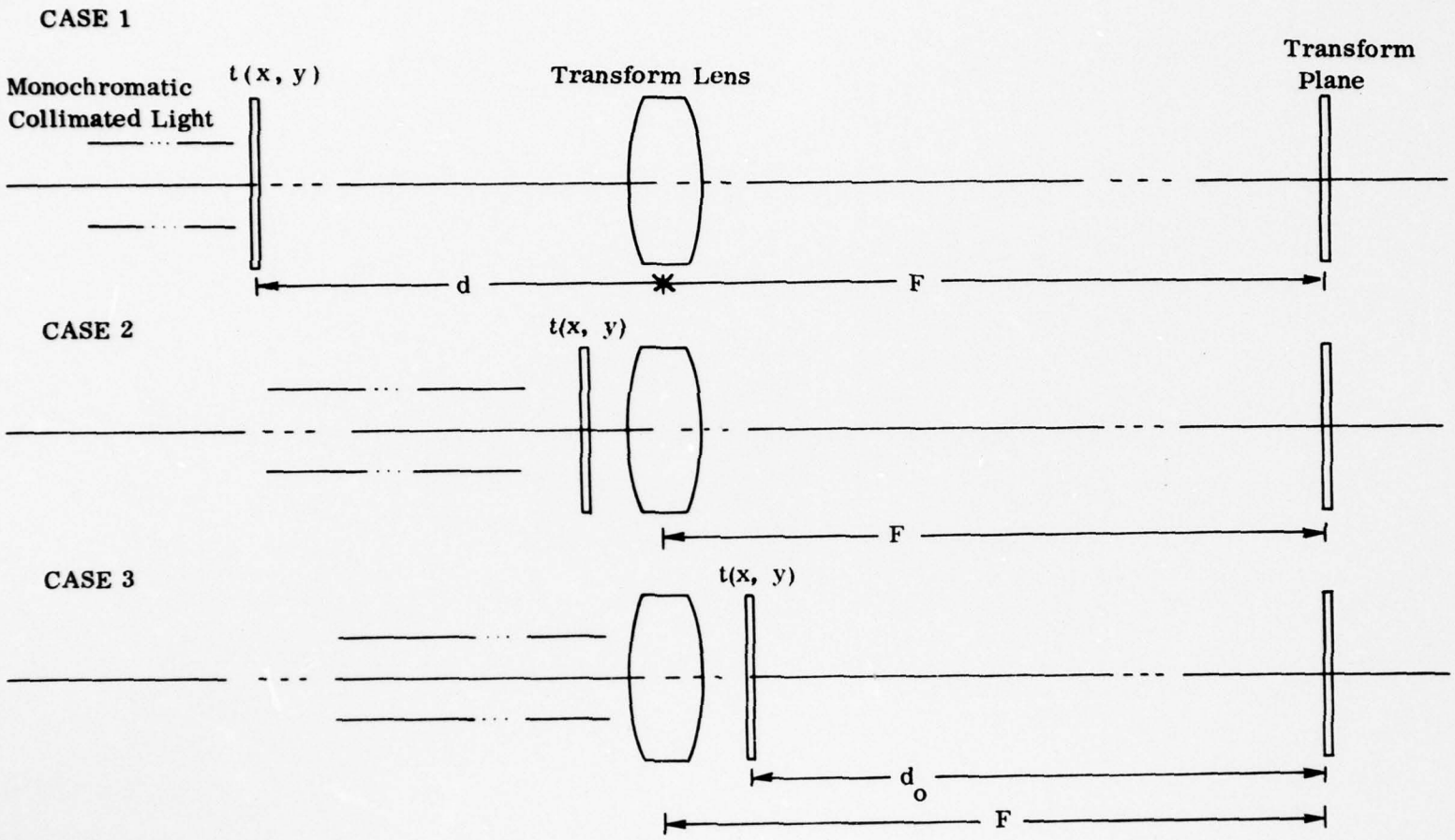

Figure 2-1. Fourier Transform Configurations

collimated monochromatic light. The amplitude distribution produced at the back focal plane of the lens is related to the two-dimensional Fourier transform of the input transparency. In the first case the input transparency is placed at a distance d in front of the transforming lens. Using the analysis and the notation in reference (3), the amplitude distribution at the back focal plane is given by:

$$U_f(x_f, y_f) = \frac{A}{\dot{\gamma}\lambda F} \exp\left[\dot{\gamma}\frac{k}{2f}\left(1 - \frac{d}{F}\right)\left(x_f^2 + y_f^2\right)\right] \iint_{-\infty}^{\infty} t_0(x_0, y_0) \exp\left[-\dot{\gamma}\frac{2\pi}{\lambda f}(x_0 x_f + y_0 y_f)\right] dx_o\, dy_0 \tag{2.1}$$

where $t_o(x_0, y_0)$ is the amplitude transmittance of the input transparency and the coordinate system is defined in Figure 2-2. The finite extent of the lens is neglected in the above expression. When d = F or when the input transparency is placed exactly at the front focal plane of the lens, the amplitude distribution corresponds exactly to the two-dimensional Fourier transform of the object.

In the second case, the amplitude in the back focal plane is given by

$$U_f(x_f, y_f) = \frac{A}{\dot{\gamma}\lambda F} \exp\left[\left(\dot{\gamma}\frac{k}{2F}\left(x_f^2 + y_f^2\right)\right)\right] \iint_{-\infty}^{\infty} t_0(x, y) \exp\left[-\dot{\gamma}\frac{k}{2F}(x\, x_f + y\, y_f)\right] dx\, dy \tag{2.2}$$

This again shows that the amplitude distribution is related to the two-dimensional Fourier transform except for a quadratic phase factor.

In the third case, the amplitude in the back focal plane is given by

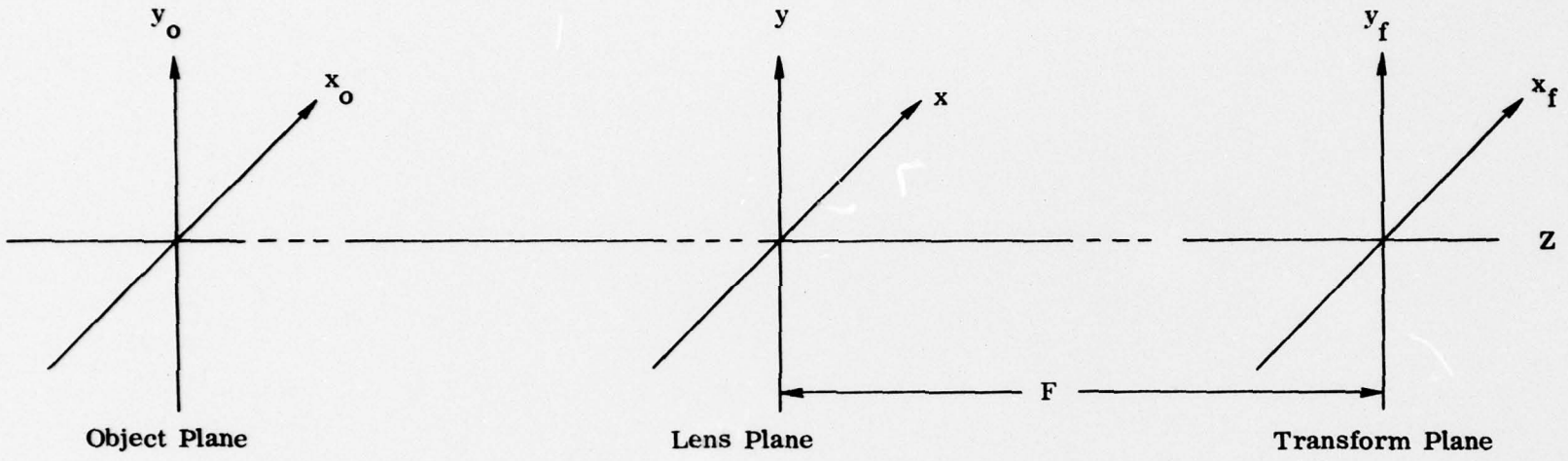

Figure 2-2. Coordinate System Definition

$$U_f(x_f, y_f) = \frac{AF}{\dot{\gamma}\lambda d_0^2} \exp\left[\dot{\gamma} \frac{k}{2d_0} (x_f^2 + y_f^2)\right]$$

$$\iint_{-\infty}^{\infty} t_0 (x_0, y_0) \exp\left[-\frac{\dot{\gamma}k}{2d_0} (x_0 x_f + y_0 y_f)\right] dx_0\, dy_0 \qquad (2.3)$$

For optical power spectrum measurement, the intensity distribution $\left|U_f(x_f, y_f)\right|^2$ in the back focal plane is measured. Hence the phase factor differences associated with the three cases presented are not recorded. The distribution in the third case differs from the first case by a scale factor determined by $(\frac{d_0}{F})$. The spatial frequencies in the first two cases are defined by the focal length F and is given by $F_x = \frac{x_f}{\lambda F}$ and $F_y = \frac{y_f}{\lambda F}$. For the third case the spatial frequencies are defined by distance d_0 and is given by $F_x = \frac{x_f}{\lambda d_0}$ and $F_y = \frac{y_f}{\lambda d_0}$.

The intensity distribution at the back focal plane is referred to as the intensity diffraction pattern, Wiener spectrum or optical power spectrum. The measurement of the intensity distribution at the back focal plane permits spectral analysis of the spatial signal represented by the transparency in the input plane and this forms the basis for all optical power spectrum analyses.

2.3 OPS Applications

During early stages of development of coherent optical processing, the application of optical power spectrum measurement and analysis was largely directed towards processing one-dimensional time signals (5,6,7,8). Usually the time signal is presented to the optical system in two ways. In the first case, the time varying signal is recorded on film with light amplitude transmittance of the film along its length proportional to the amplitude of the original time signal. The most popular way in recent times is to use acousto-optic cells to convert the time signal to a spatial signal. Using better materials and fabrication techniques the performance of the acousto-optic cells has been considerably increased enabling the optical power spectrum analyses of wideband signals attractive and

highly desirable (9, 10). As the time signal is applied to the acousto-optic cell, an acoustic signal propogates within the acousto-optic material. This acoustic wave phase modulates the transmitted light. Fourier transforming this spatially modulated signal in an optical power spectral analyzer permits realtime spectral analysis of the time signal.

The use of optical power spectral analysis to process two-dimensional spatial signals has many applications (11, 12, 13). Its use in pattern recognition, image assessment and feature classification has been demonstrated by several investigators. Custom configured two-dimensional optical power spectrum measurement systems are commercially available and are being applied to a variety of special applications. It is in this context that the description of the HOPS system is presented in this report.

2.4 Commercial OPS Systems

There are two commercially available OPS measurement systems; the Recording Optical Spectrum Analyzer (ROSA) that is available from Recognition Systems, Inc., and the Diffraction Pattern Analyzer, available from EIKONIX Corp. Both systems are similar as far as their optical configuration is concerned but they differ in their modes of measurement and processing.

The ROSA System consists of three subsystems; the coherent optical subsystem, the detection and recording subsystem associated with the detector and the computer, and the related pattern recognition software as shown in Figure 2-3. In the coherent optical subsystem, a 5 mw He-Ne laser provides a coherent beam which is scaled in amplitude by a variable attenuator prior to filtering with a pinhole spatial filter and beam expansion with a collimator assembly. The collimated output beam illuminates the transparency. A wheel containing circular apertures permits the definition of a sampling aperture on the plane of the transparency. It can be varied from 0.125" to 3" diameter. The transform lens placed behind the transparency produces the power spectral

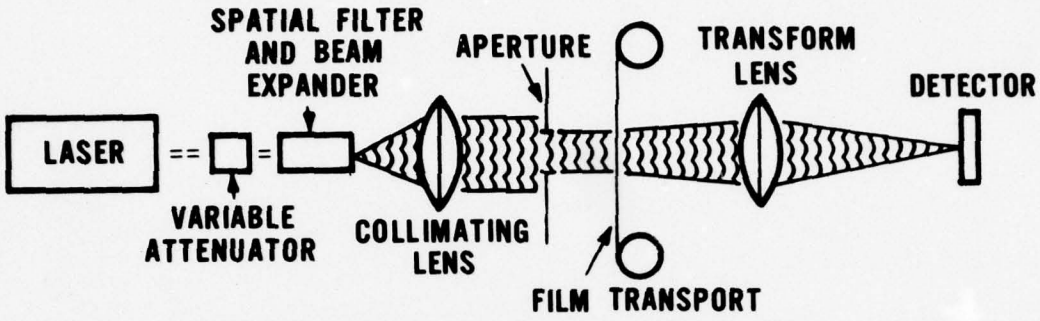

A. COHERENT OPTICAL SYSTEM CONFIGURATION

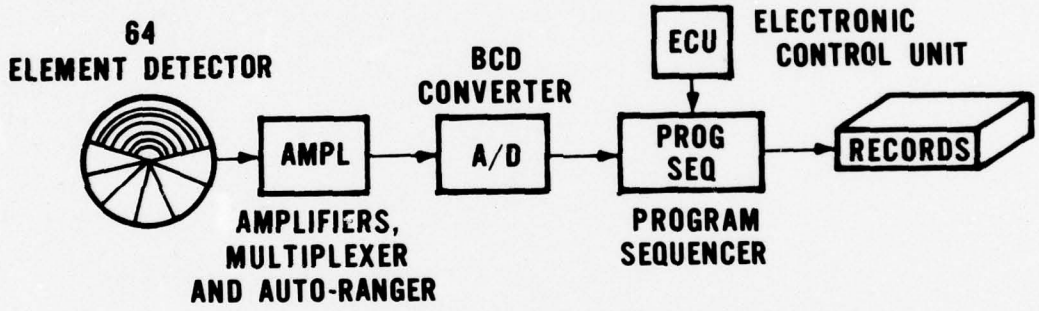

B. ELECTRONIC PROCESSING AND RECORD SYSTEM

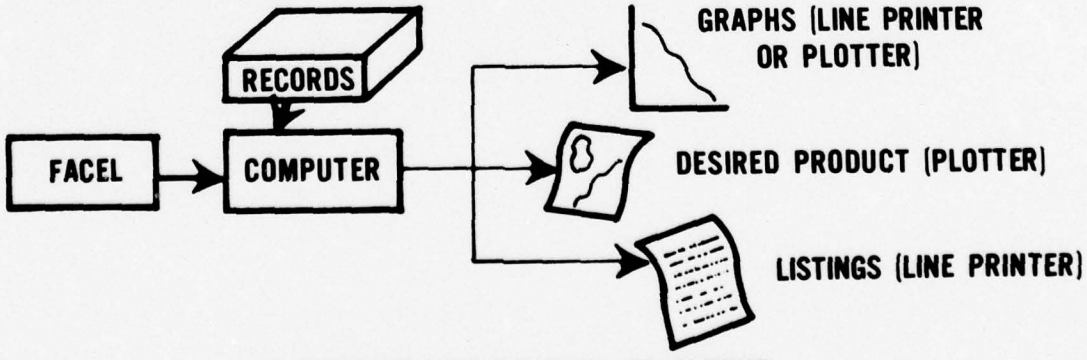

C. SOFTWARE PROCESSING AND OUTPUT

Figure 2-3. ROSA System

distribution on the plane of the detector. The segmented photodetector used to sample the intensity distribution makes use of the symmetric nature of the power spectral distribution. The segmented photodetector is illustrated in Figure 2-4. The 32 ring segments in one half plane permits the measurement of the intensity distribution as a function of the radius (or frequency) and the 32 wedge segments in the other half plane permit the measurement of the intensity distribution as a function of the polar angle θ. The electric signals from each of the detector elements are processed through individual amplifiers and then multiplexed to an auto-ranging amplifier. The analog signals are then converted to digital form to be processed in the computer. Leighty and Lukes (14) have characterized the performance of the ROSA optical and electronic processing systems for mapping applications.

The Diffraction Pattern Analyzer made by EIKONIX Corporation differs from the ROSA in its method of detection of the power spectral distribution. It is also designed and configured for use by an operator evaluating roll or chip transparencies on a light table. The system configuration of a particular design of the EIKONIX system is illustrated in Figure 2-5. A zoom microscope with a camera is available for detailed inspection and recording of the image samples. Eleven circular apertures ranging from 1 mm to 30 mm can be selected to define the sampling area on the plane of the transparency. A set of annular masks are sequentially positioned in the spatial frequency plane for sampling the power spectral distribution. The energy passing each filter is collected and detected with a photomultiplier tube. The signals are subsequently amplified, digitized and then recorded. The system automatically sequences and positions up to 20 annular masks specified by the operator for the OPS measurement at each sample point in the input image. A rotating slit behind the annular masks permits sampling of the angular distribution of the power spectral distribution. Thus, the combination of annular masks and the rotating slit permits the measurement of the power spectral distribution in polar coordinate form over the entire frequency plane.

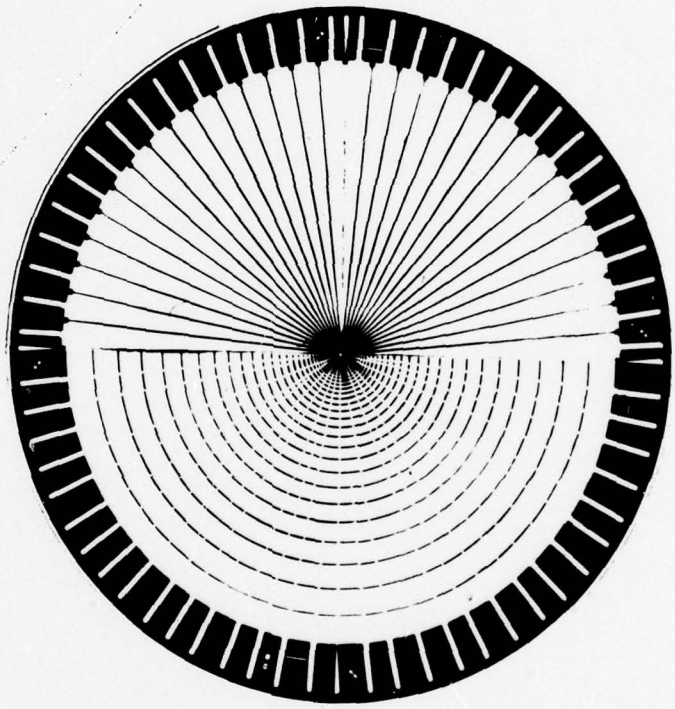

Figure 2.4 Segmented RSI Detector

POWER SPECTRUM ANALYZER MODEL EC-742
BLOCK DIAGRAM

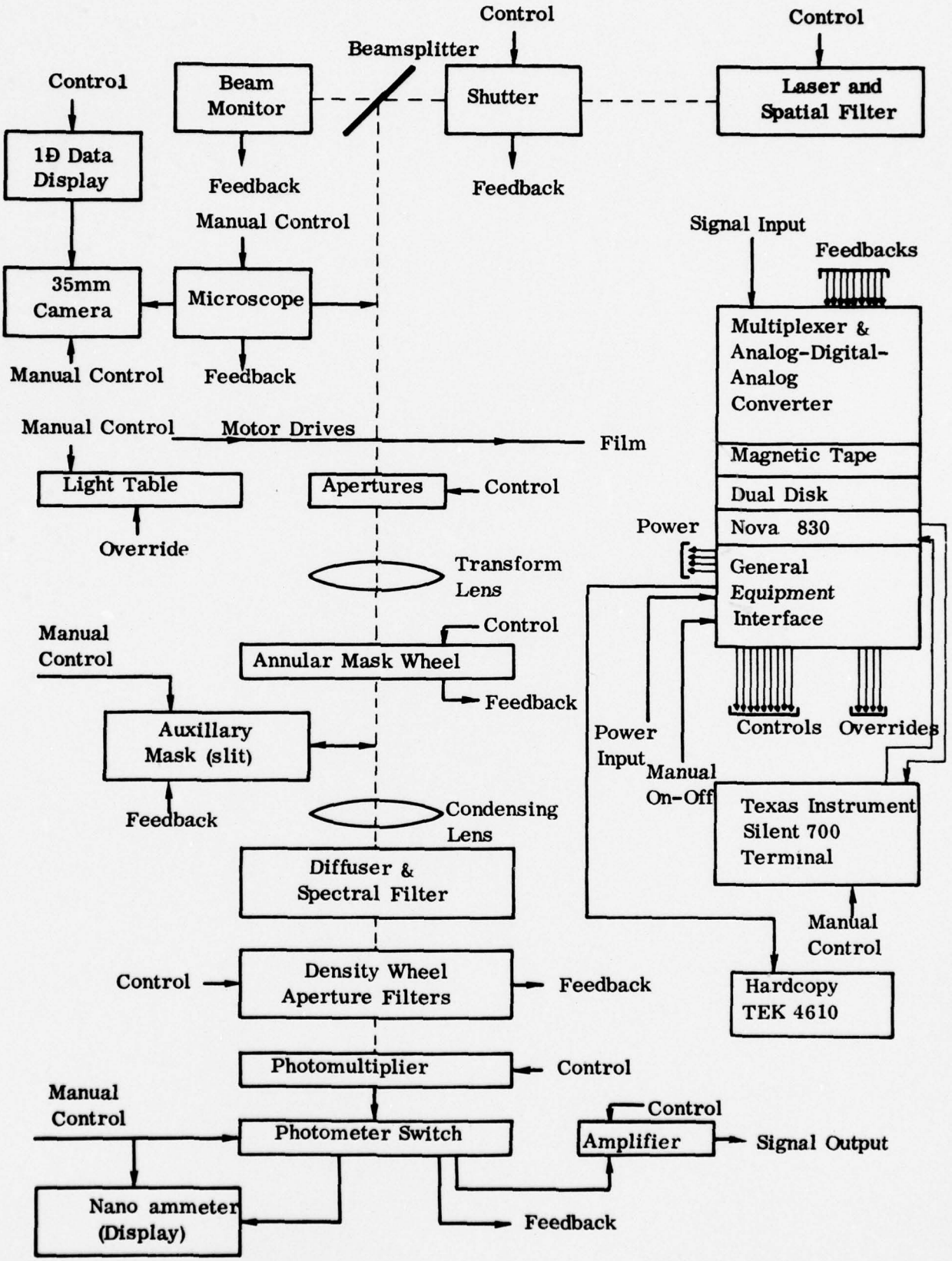

Figure 2-5 Block Diagram of the EIKONIX Power Spectrum Analyzer

2.5 Evaluation

Many of the mapping applications of OPS analysis require rapid sampling over large two-dimensional aerial transparency formats. For the systems described above, this can be accomplished either by the translation of the film over the sampling aperture or by direct or apparent translation of the sampling aperture over the film format. The mechanical translation of the film transport or the film holder over the sampling aperture is cumbersome and slow. Recent advances in laser scanning techniques have made the apparent translation of the sampling aperture over the stationary film format viable and attractive. Several large format scanning systems have been proposed and demonstrated (15). Figure 2-6 illustrates one example of an OPS measurement system incorporating the scanning concept.

In evaluating the existing OPS measurement systems for mapping applications, one must take into consideration the means for implementing rapid sampling over large format input transparencies. It is in this context that the two OPS measurement systems described above have operational disadvantages.

The Fourier transform distribution at the back focal plane represents the convolution of the object transform and aperture transform. Whenever a very small sampling aperture is desired, the effect of the convolution process is to considerably smooth the resulting power spectral distribution. Also, because of the large optical path length associated with the optical scanning systems, a small sampling aperture may not be well resolved at the transparency plane. In addition, the smaller sampling apertures require higher scanning rates to scan equivalent film areas as larger sampling apertures.

Another design consideration is the complexity of the laser scanner comparison to the approach presented here. The HOPS (high resolution optical power spectrum analyzer) measurement scheme presented in this report is an attempt to overcome these specific problems associated with the practical

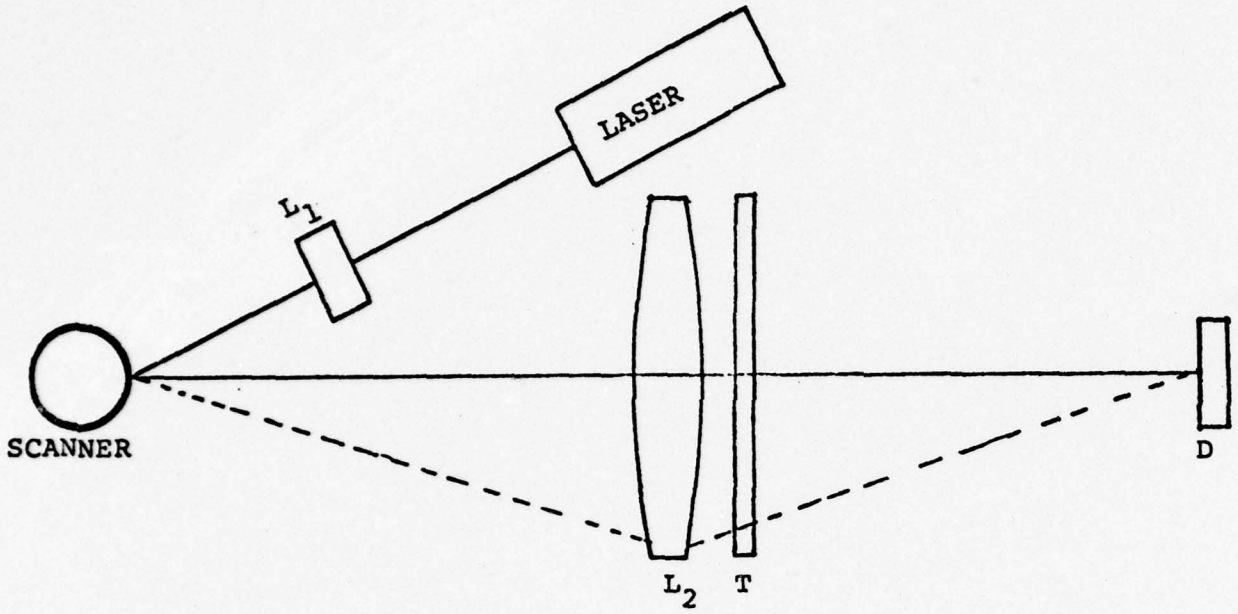

Figure 2-6. Laser Scanner Based OPS Measurement System

implementation of "conventional" OPS measurement systems. (Additional design considerations associated with the OPS measurement systems are presented in Appendix A.)

3. HIGH RESOLUTION OPTICAL POWER SPECTRUM ANALYZER

3.1 Introduction

The discussion presented in the previous chapter indicates some problems associated with "conventional" optical power spectrum measurement systems whenever the sample apertures become small. In this chapter a different system configuration for optical power spectrum measurement, one that is ideally suited for high resolution applications, is described. The basic principle of operation is presented and the image characteristics of the system configuration are outlined. Analytical evaluation is presented to show the potentials and the limits of this approach to optical power spectrum analysis.

3.2 Principles of Operation

The optical configuration of the high resolution optical power spectrum analyzer (HOPS) is illustrated in Figure 3-1. The light from the laser is spatially filtered and expanded to illuminate the transparency under examination. A converging beam illuminates the transparency and produces at the plane containing the point of convergence, an amplitude distribution that is related to the Fourier transform of the input transparency. An imaging lens placed just behind the transform plane forms an image of the transparency on a detector array. By means of this design approach, each element of the detector array projected back onto the plane of the transparency defines a sampling aperture. A spatial filter mask placed in the transform plane permits the power contained in that spectral band to reach the final image. The output of each element of the detector array is then proportional to the sampled power spectrum of the corresponding sampling aperture. In order to sample the power spectrum completely, different spatial filtering masks are introduced at the transform plane. This represents a simplified explanation of the HOPS measurement concept.

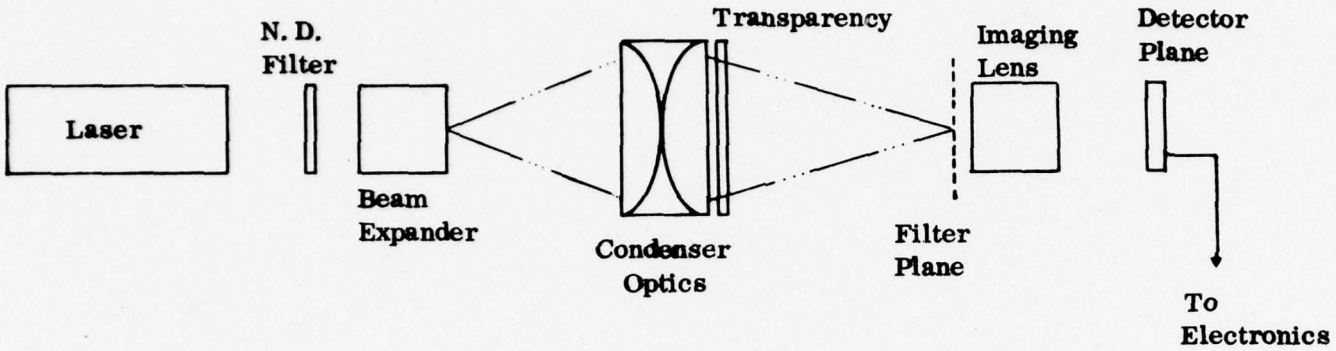

Figure 3-1. Basic HOPS Measurement System

There are two approaches for realization of HOPS. They are illustrated in Figure 3-2 and are:

a. HOPS with Two-Dimensional Array Detector

b. HOPS with One-dimensional Array Detector

The two-dimensional detector design samples a full-two-dimensional transparency format as illustrated in Figure 3-2(a). The transparency is positioned in the optical system and the transform filters are sequentially introduced at the transform plane for the OPSA measurements. The film is stepped to the next frame for its measurement. With the one-dimensional detector design (Figure 3-2(b)), the transparency continuously moves through sampling gates and sequential optical detectors extract the power spectrum samples. Most of the experimental effort of this program was applied to the first design approach. The second is described in Chapter 4, where both are evaluated and compared.

By means of the basic HOPS concept, a spatially filtered image is sampled by the detector array and the spatial filtering takes place for the entire image as a whole. However, the individual elemental areas defined by the detector aperture are not independent. It is in this context that the power spectrum measured using the HOPS measurement concept is distinctly different from the "conventional" OPS measurement schemes.

Considering the basic HOPS configuration shown in Figure 3-1; the imaging lens forms an image of the transparency at the plane of the detector. For the purposes of this analytic treatment, let us assume that the imaging lens forms an image at 1:1 magnification and the impulse response of the imaging lens is a delta function. This assumption permits one to assume that with no spatial filters present in the system, the amplitude distribution at the detector plane is given by the amplitude transmittance of the transparency $t(x, y)$. If $S(f_x, f_y)$ is the amplitude transmittance of the spatial filter at the transform plane, the amplitude distribution $U(x_i, y_i)$ at the image plane is given by

$$U(x_i, y_i) = \int_{-\infty}^{\infty}\int t(x, y)\, S(x_i - x, y_i - y)\, dx\, dy \qquad (3.1)$$

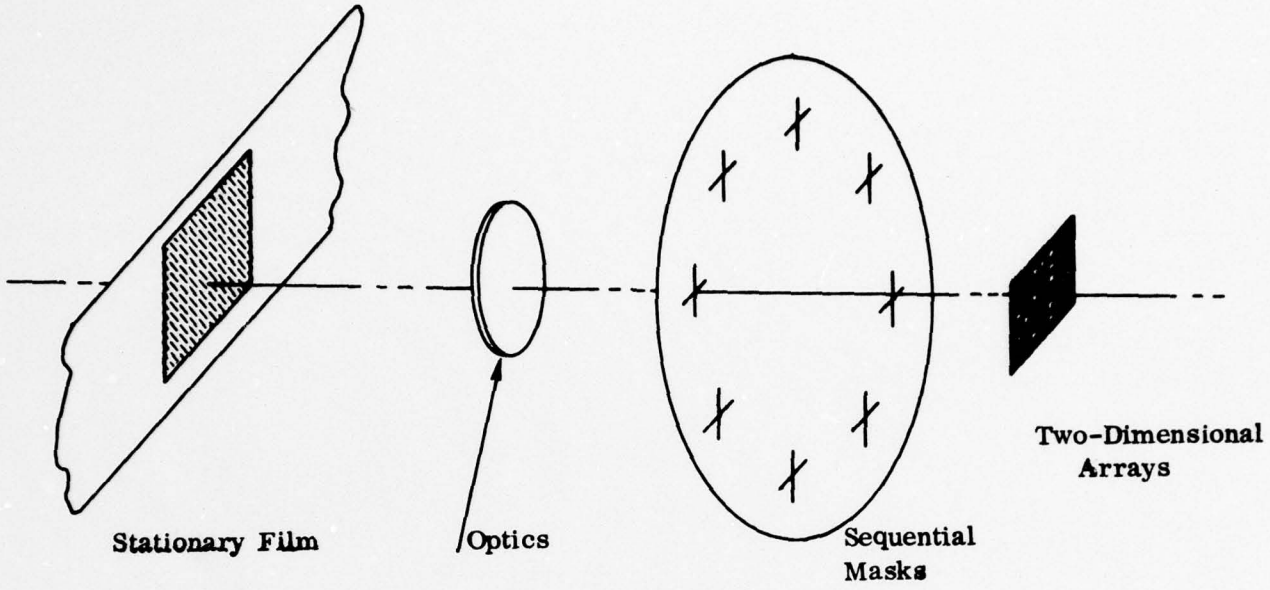

(a)

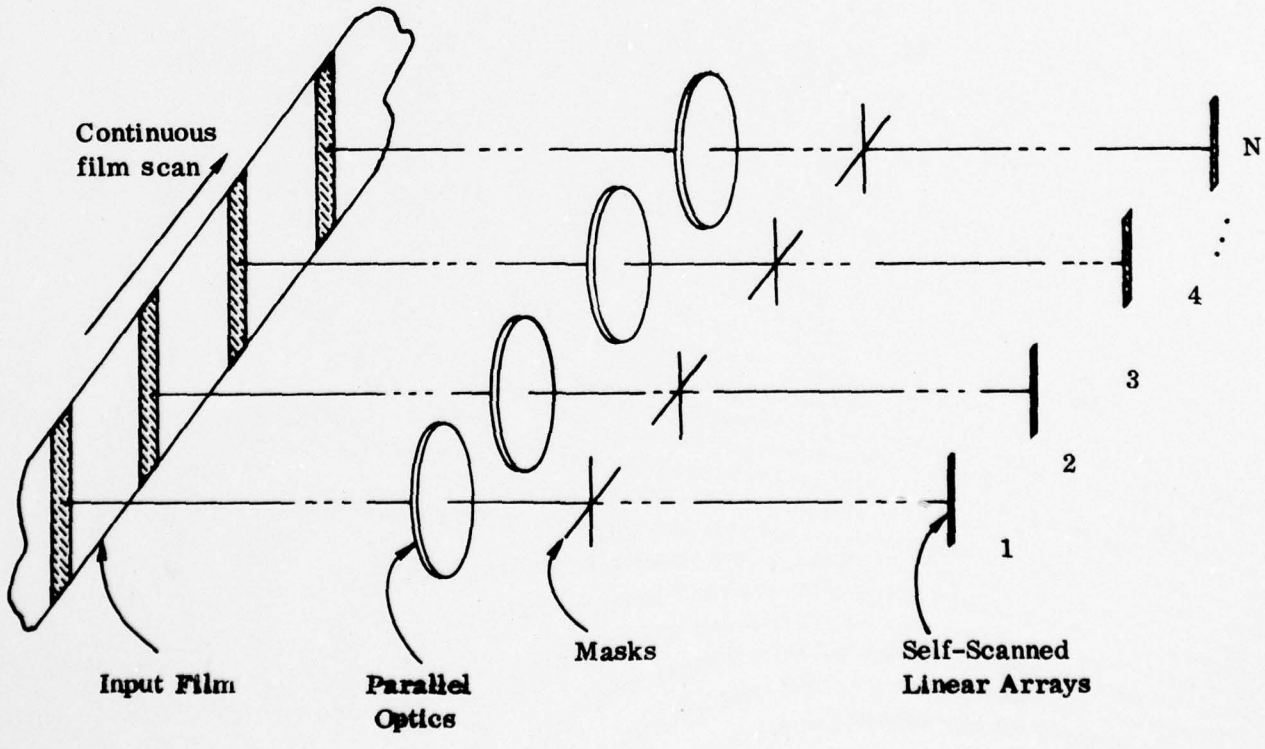

(b)

Figure 3-2. HOPS Design Approaches, with a Two-Dimensional Detector Array (a), and a One-Dimensional Detector Array (b)

where $S(x_i, y_i)$ is the Fourier transform of $S(f_x, f_y)$. This can also be expressed by:

$$U(x_i, y_i) = t(x_i, y_i) * S(x_i, y_i) \tag{3.2}$$

where * represents convolution. The elemental detector output $I_0(n, m)$ is given by

$$I_0(n, m) = k \int_{-\infty}^{\infty} A(x_n - x_i, y_m - y_i) \left| U(x_i, y_i) \right|^2 dx_i\, dy_i \tag{3.3}$$

where (n, m) defines the matrix of the detector array, k is a constant dependent on the detector characteristics and $A(x_n - x_i, y_m - y_i)$ is the detector aperture function for the element centered at (x_n, y_m).

Substituting for $U(x_i, y_i)$ equation (3.3) becomes

$$I_0(n, m) = k \int_{-\infty}^{\infty} A(x_n - x_i, y_m - y_i) \left| t(x_i y_i) * S(x_i, y_i) \right|^2 dx_i\, dy_i \tag{3.4}$$

The above expression clearly defines the measurement made in the HOPS configuration. In words, the measured data represents the integral of the spatially filtered intensity image over the detector aperture placed in the image plane. On the basis of Parseval's theorem (16), this can be easily related to the power spectra measured in the transform plane. However the difficulty arises when one tries to define the aperture on the original input transparency to which the power spectral measurement is associated. This statement can be elaborated by considering the properties associated with Fourier transform pairs. If f(x) and $F(\omega)$ are Fourier transform pairs, then if $F(\omega)$ is band limited in such a way that

$$F_a(\omega) = \begin{cases} F(\omega), & |\omega| \leq a \\ 0, & |\omega| > a \end{cases}$$

then

$$f_a(x) = f(x) * \frac{\text{Sin } a\,x}{\pi x} \tag{3.5}$$

of if f(x) is space limited in such a way that

$$f(x) = \begin{cases} f(x), & |x| \leq a \\ 0, & |x| > a \end{cases}$$

then

$$F_a(\omega) = F(\omega) * \frac{\text{Sin } a\,\omega}{\pi\,\omega} \tag{3.6}$$

Hence, the frequency spectrum is band limited, then its Fourier transform $f_a(x)$ must be continuous. According to the uncertainty principle (16), the product of the widths of the space function and its Fourier transform cannot be less than a certain minimum value ($\sqrt{\pi E}$, E being the total energy in the signal).

The defintion of the sampling aperture on the plane of the transparency for which the OPS measurement has been made is dependent on the bandwidth associated with the spatial filtering masks. The uncertainty in the definition of the aperture function becomes reduced as the bandwidth associated with the spatial filtering masks is increased. The effect of the spatial filter bandwidth on the final image can be illustrated by numerical calculation. For the purpose of simplicity and ease of calculation, the example is restricted to one-dimensional signals. The results of the numerical calculation are illustrated in Figure 3-3. The graph shown in (a) represents the input signal. The plots shown in (b), (c), (d), (e), and (f) show the filtered first harmonic of the signal, with varying filter

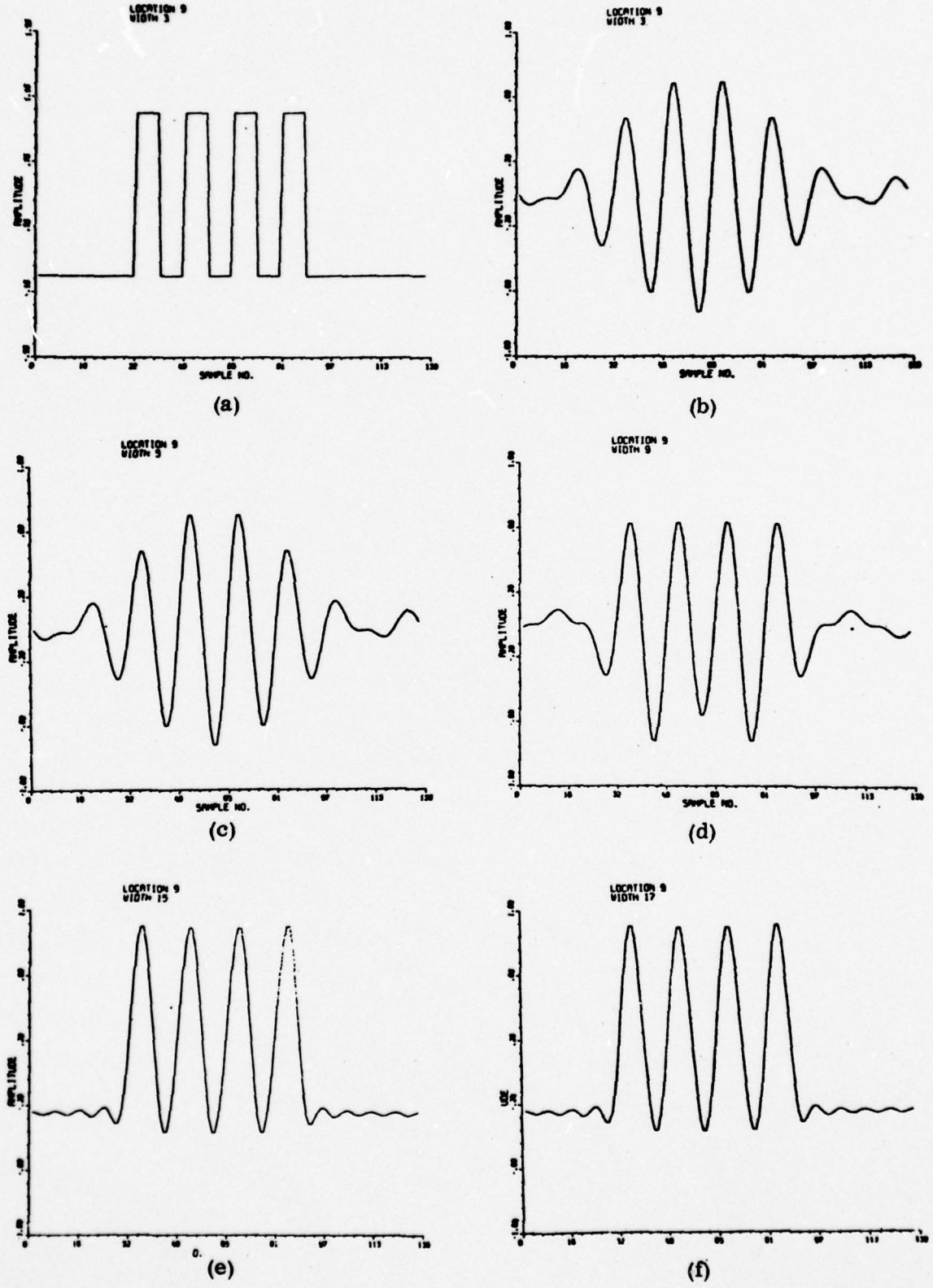

Figure 3-3. Effect of Spatial Filter Bandwidth

filter bandwidths. The bandwidths increase from (b) to (f). The convolution effects due to the filter are clearly illustrated, having greatest impact in plots (b) and (c).

3.3 Differences with Conventional OPS Measurement Systems:

In the conventioanal OPS systems the measurement is made in the transform plane and the sampling aperture is defined in the input transparency plane. A photo detector having an aperture $D(f_x, f_y)$ permits sampling of the frequency distribution at the transform plane. The spatial frequency bandwith associated with detection is determined by the width of the detector aperture $D(f_x, f_y)$. The output of the detector, when it is placed at any specific center frequency (f_{xn}, f_{yn}), is given by

$$I_0(f_{xn}, f_{yn}) = k\int_{-\infty}^{\infty}\int\left|T(f_x, f_y) * A(f_x, f_y)\right|^2 \cdot D(f_{xn} + f_x, f_{yn} + f_y)\, df_x\, df_y \tag{3.7}$$

where k is a constant dependent on the detector characteristics. $T(f_x, f_y)$ is the Fourier transform of the input transparency $t(x, y)$ and $A(f_x, f_y)$ is the Fourier transform of the sampling aperture $a(x, y)$. In the direct OPS measurement, the power contained within a spectral band is measured for a sample aperture of the imagery. The sampling aperture $a(x, y)$ is well-defined at the plane of the transparency. The Fourier transform of the input transparency is convolved with the aperture transform, resulting in a smoothed final distribution shown in Equation (3.7). The smaller the sampling aperture $a(x, y)$, the greater the smoothing of the final transform distribution. Hence one of the major differences between the direct OPS measurement and the HOPS measurement lies in the definition of the measured data. In the direct OPS measurement scheme, the sample aperture is clearly defined at the expense of an uncertainty in the definition of the measured frequency distribution. In the HOPS measurement, the convolution effects due to the aperture of the transparency can be considered negligible and hence the measured

frequency is well defined at the expense of an uncertainty in the definition of the sample aperture at the plane of the transparency. This difference between the two measurement schemes becomes negligible as either the sample aperture in the plane of the transparency or the measurement spatial frequency bandwidth or both are made reasonably large.

3.4 Unique Characteristics

There are distinct advantages to the HOPS measurement scheme. The unique characteristics of this measurement approach are:

a. The location of the sampling aperture in the final image plane permits the use of self-scanning diode arrays to cover and sample the transparency. This is particularly advantageous whenever large input formats are involved since it overcomes problems associated with scanning systems.

b. The sampling apertures can be made small depending upon the spectral width of the spatial filters and this permits high resolution sampling at the plane of the transparency.

c. Depending upon the number of detector elements and the number of spatial filter masks, the system speed can be very high.

d. For applications involving large input formats, compared with laser scanning OPS systems, HOPS can be designed to be compact and more stable to withstand adverse environmental conditions.

3.5 Experimental Demonstration

The experimental arrangement used for the demonstration of the HOPS concept is illustrated in Figure 3-4. A photograph of the experimental setup is shown in Figure 3-5. Light from a 6 mW He-Ne laser (CR-80-6) is used to provide a point source using the microscope objective-pinhole spatial filter combination. A neutral density filter placed between the laser and the microscope

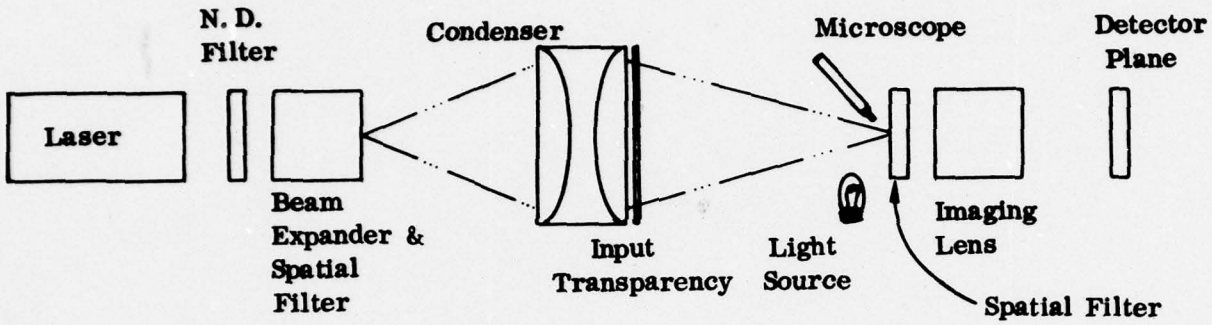

Figure 3-4. Experimental HOPS Configuration

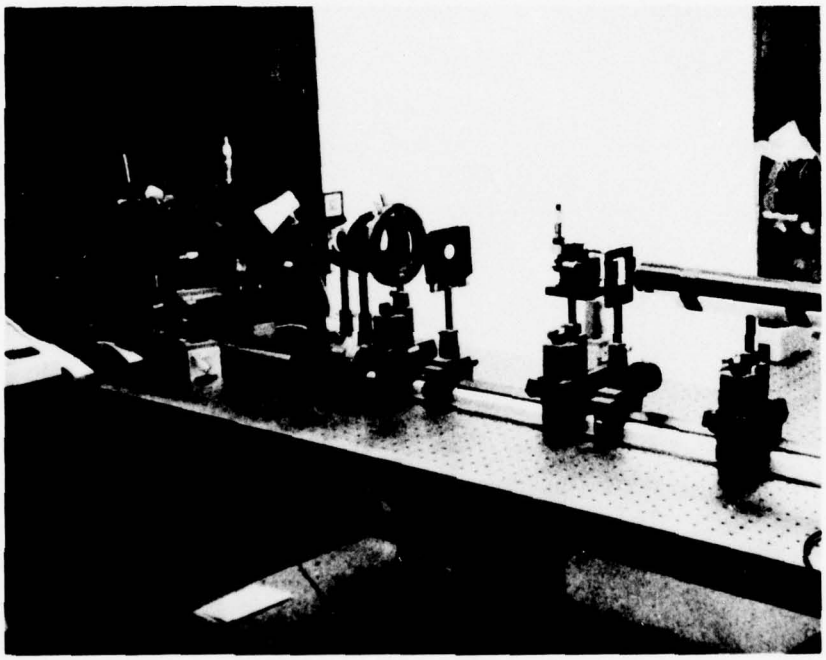

Figure 3-5. Experimental HOPS Set-Up

objective permits attenuation of the laser power. Two collimator objectives, mounted back-to-back, image the source defined by the pinhole spatial filter near the entrance aperture of the imaging lens and in the process provide a converging spherical beam to illuminate the input transparency as shown in Figure 3-4. The spatial filtering masks are placed in the plane containing the image of the pinhole-spatial filter, just in front of the entrance aperture of the imaging lens. The aperture of the imaging lens is selected to be large enough to make the spatial filtering masks the limiting aperture. The holder containing the spatial filter is mounted on an XYZ translation stage so as to permit centering of the spatial filter masks with respect to the optical axis of the system (actually with respect to the d.c. spot of the power spectrum). During the alignment process, the mask is illuminated from the side by a tungsten light source and with the help of an observation microscope, the masks are positioned accurately. The reticles of the microscope and the bright d.c. laser spot of the power spectrum are used as references in aligning the masks.

The image plane of the input transparency formed by the imaging lens represents the measurement plane. This plane is occupied by either recording film or a detector array depending upon the nature of the measurement made. When a photographic film is used, a 35 mm back is utilized as a film holder and the view finder associated with the back permits alignment of the final image on the film plane. When the detector array is used, an examination of the video signal from the detector array on an oscilloscope (to obtain high modulation signal) helps in aligning the detector plane to coincide with the image plane.

The detector array used for this first experimental HOPS demonstration was a Reticon 32x32 two-dimensional array, the performance characteristics of which are outlined in Table 3-1. The block diagram in Figure 3-6 explains the data extraction electronics used to output the measured data from the diode array. Figure 3-7 shows a photograph of the photodiode array and the related electronics.

Table 3-1

Characteristics of Reticon Array

SPECIFICATIONS

ELECTRICAL CHARACTERISTICS (25°C)
(Voltages with respect to common)

	Min	Typ	Max	Units
Video Output line Bias		-5	-8	Volts
Supply Voltage V_{DD}	-11	-12	-13	Volts
Clock Pulse Amplitude	-11	-12	-13	Volts
Start Pulse Amplitude	-7.5	-10	-13	Volts
Start Pulse Width	1/f[1]		[2]	Sec
End of line/frame output resistance		5		K ohms
End of line output pulse width		2/f[1]		Sec
Video line capacitance (at -5 volts)				
RA-50x50A		220		pf
RA-32x32A		105		pf
Diode Sample Rate				
RA-50x50A	$5x10^4$		$5x10^6$	Hz
RA-32x32A	$2x10^4$		$5x10^6$	Hz
Frame Rate				
RA-50x50A	20		2000	Hz
RA-32x32A	20		2000	Hz
Power Dissipation (DC)		10		m watt

ELECTRO-OPTICAL CHARACTERISTICS (25°C)

Photodiode sensitivity[3]	250		pA/ft-cd
	5		pA/μwatt/cm²
Uniformity of sensitivity[3-4]	±10		%
Saturation Exposure[3]	$6x10^{-3}$		ft-cd sec
	.32		(μwatt/cm²) sec
Saturation charge (at -5 volts)	1.6		pcoul

MECHANICAL CHARACTERISTICS

Number of diodes			
RA-50x50A	2500		
RA-32x32A	1024		
Number of rows and columns			
RA-50x50A	50		
RA-32x32A	32		
Spacing (row and column)	4		Mils
Diode sensing area	8		Mils²
Package size (16 pin DIP)	0.6x0.8		inch

ABSOLUTE MAXIMUM RATING

Voltage with respect to common	0	-20	Volts
Storage temperature	-55	+85	°C
Temperature under bias	-55	+85	°C

NOTES:
[1] = diode sample rate
[2] = self-starting beyond 34/f for 32x32 or 52/f for 50x50
[3] 2870°K tungsten source
[4] Negelects first and last elements of each line

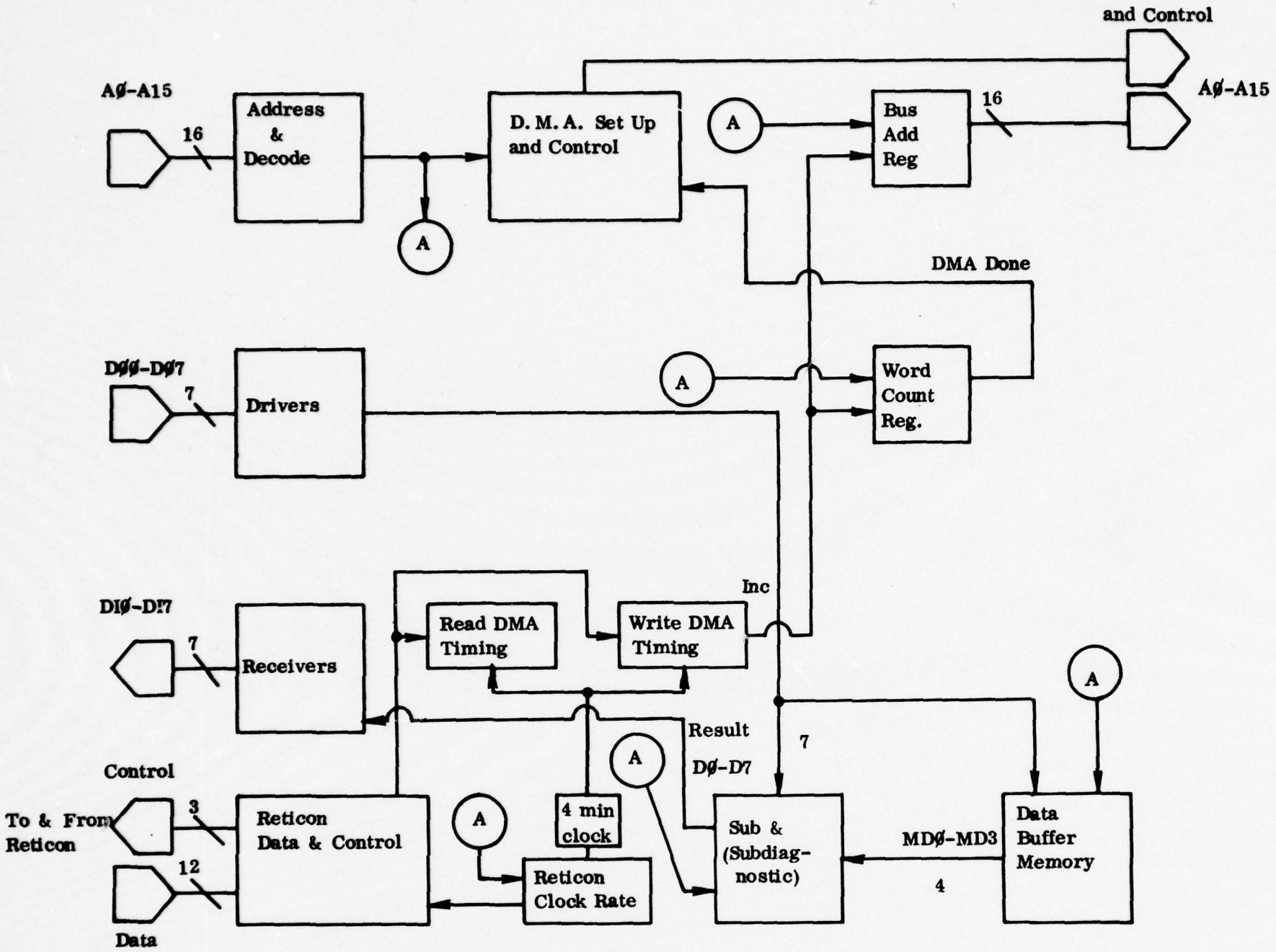

Figure 3-6. Block Diagram of Data Extraction Electronics

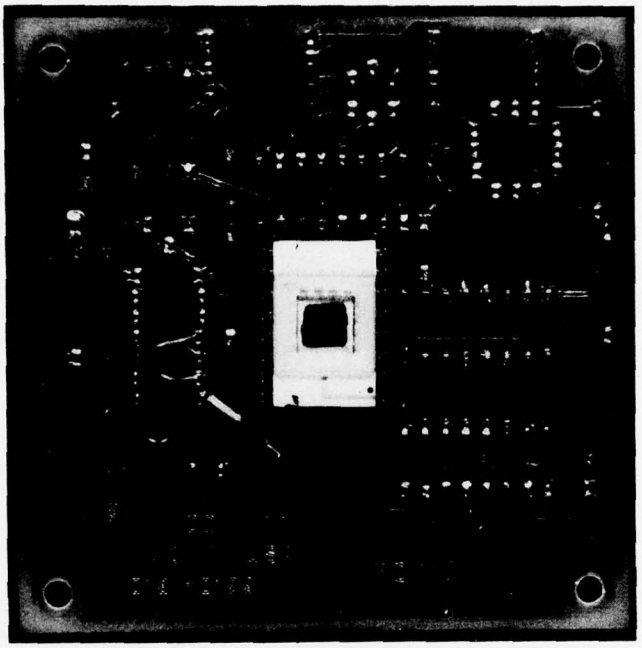

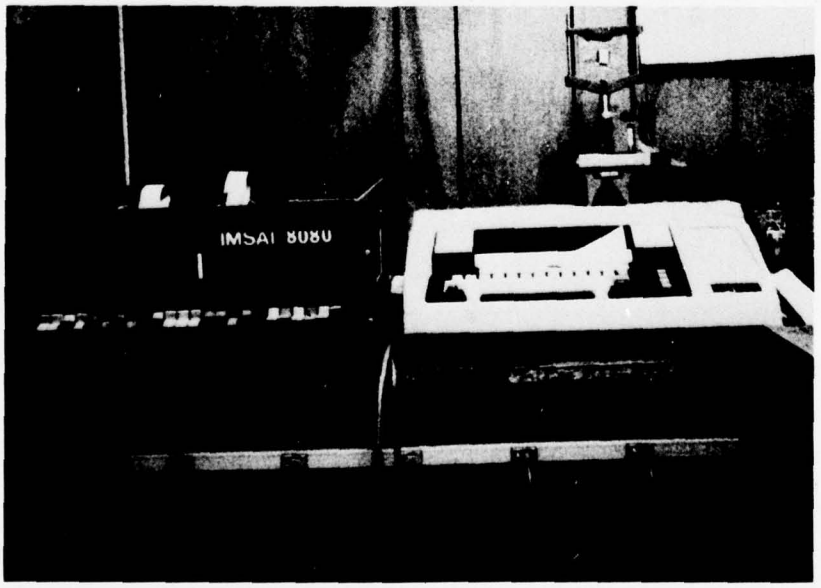

Figure 3-7. Photograph of the Array and the Associated Electronics

3.5.1 Data Extraction Electronics

The data extraction electronics consists of a D.M.A., Reticon, dark buffer, subtractor, and control electronics. The D.M. A. (Direct Memory Access) electronics permits the Reticon data to be transferred to memory directly without microprocessor intervention. This method of data transfer simplifies software and has a high data transfer rate.

The Reticon electronics receives the Reticon data at a rate proportional to the programmed pre-setable Reticon clock. The dark buffer memory stores the dark current of the Reticon via program control once per day. The dark buffer memory has a 1K by 5 bit organization. With the micro-processor being the associated control electronics, dark buffer data is subtracted from the input Reticon data on the fly, and under D.M.A. control. The entire data extraction electronics is controlled via micro-processor software.

Under program control the dark buffer memory is initialized to zero and a Reticon scan is performed with no room light. The dark current data is stored in the micro-computer, and also under program control, is transferred to the dark buffer in the extraction electronics. When a normal scan is performed, the data from the Reticon has the dark current subtracted on the fly and the results are stored in memory (1K bytes) and subsequently transmitted to a printer. The data output is printed on a Texas Instrument Silent 700 printer in a special format (8 column by 32 rows) x 4 so that a 32 row by 32 column can be constructed.

3.5.2 Detector Dynamic Range

During the initial phase of this investigation, considerable attention was given to the applicablility of commercially available detector arrays as the detector for the HOPS system. The particular detection requirement that is of importance to HOPS is the dynamic range of the signal. In most applications in mapping involving aerial photography, the dynamic range required for power

spectral measurement is about 10^4. Photodiode detector arrays are not capable of providing that kind of dynamic range. However, for the purposes of HOPS measurement, the measurement dynamic range of the diode array can be artificially increased by several ways. In the first case a sequence of measurements can be made with increasing laser power and the data normalized subsequently with the laser power. During each measurement only the data that lies within the measurement dynamic range of the detector array is recorded. If the detector array has a dynamic range of 100 and if the laser power can be attenuated by a factor of 100 (N D = 2), then a measurement dynamic range of 10^4 can be obtained. A second way to increase dynamic range is by means of scan rate control. The self scanning Reticon array is an integrating photodetector, the time of integration being determined by the scan rate. A scan rate difference of a factor of 100 extends the dynamic range by that amount. A third way to increase the system dynamic range is to use ND filters in the spectrum sampling masks to reduce the power spectrum dynamic range. The subsequent requirements for adjustment of data is exactly the same as the first case.

3.5.3 HOPS Tests

Experiments were performed to evaluate the HOPS measurement concept. In the first test a photometer was used as the photodetector and, using an aperture in the image plane, the elemental detector of the diode array was simulated. This was compared with conventional OPS measurements; this test is described below. A second test evaluated a "one shot" spectrum filter in the HOPS. This enables an analog equivalent of a first moment weighting of the OPS, and removes the requirement for sequential spectrum sampling. In the third test, film was substituted for the Reticon two-dimensional array, for demonstration in the HOPS recorder. The two-dimensional self-scanned array had limitations that prohibited large dynamic range scanning. This problem is overcome with one-dimensional arrays as described in the fourth test.

TEST NO. 1 In the first experimental test, power spectrum measurements were made using both the conventional and HOPS measurement approach. A sample aerial image was used as the input transparency. For the conventional OPS measurement a 5 mm diameter circular aperture was placed in the plane of the transparency and hence the illumination was limited to a selected section of the imagery that was covered by a 5 mm aperture. A narrow slit having dimensions 0.38 x 12.5 mm was used in the transform plane to sample the power spectrum of the section of the imagery illuminated. An EG & G photometer placed behind the imaging lens integrated the light passed by the slit. The EG& G photometer (Model E04G) used had a measurement dynamic range of over 10^6 and the output was presented as a digital display. The scanning slit was mounted on a translation stage described earlier and hence its position was read out from the micrometer. Because of symmetry, the measurement was restricted to one half plane. The maximum spatial frequency sampled was purely determined by the signal level associated with the OPS distribution and when it became comparable to the background noise, the measurement was terminated.

For the HOPS measurement sequence, an area much larger than the 5 mm aperture was illuminated (approximately 30 mm) and an aperture representing the image of the original 5 mm aperture was placed in the image plane. For this experimental situation, the conjugates of the imaging lens were chosen to provide 5X reduction in imaging. Hence, the aperture used in the image plane was a 1 mm diameter circular aperture. The aperture in the image plane was carefully aligned such that the same section of the image as in the conventional OPS measurement system, now filled the aperture in the image plane. The position and the scanning of the slit was the same as in the conventional OPS measurement. The scanning slit permitted spatial filtering of the entire illuminated image and the one mm aperture permitted the sampling of the corresponding spatially filtered intensity image. For exactly the same positions of the slit as in conventional OPS measurements, the readings of the photometer were recorded. The

system parameters associated with the conventional and HOPS measurement of the OPS distribution are illustrated in Figure 3-8. The results of the measurements were normalized with respect to their corresponding d. c. values and are shown in Table 3-2.

TABLE 3-2

COMPARISON OF DIRECT OPS AND HOPS MEASUREMENT DATA

Slit Position X Axis	Direct OPS Y Axis	HOPS Y Axis
0.0 mm	1.0	1.0
0.25	0.166	0.158
0.5	0.0605	0.0566
0.75	0.0428	0.0394
1.0	0.0228	0.0212
1.25	0.01352	0.0121
1.5	0.00976	0.00892
1.75	0.00747	0.00720
2.00	0.00637	0.00613
2.25	0.00536	0.005
2.50	0.00352	0.0032
2.75	0.00320	0.00305
3.00	0.00274	0.00267
3.25	0.00219	0.00215
3.5	0.00199	0.00192
3.75	0.00188	0.00182
4.00	0.00172	0.00163
4.25	0.00145	0.00146
4.5	0.00106	0.00108
4.75	0.00097	0.00091
5.0	0.00102	0.001

The data shows differences between the two measurements near the low frequency regions, that vanish near the high frequency regions. This is a direct consequence of the physical differences between two measurement techniques. In the first case, the Fourier transform was defined only with respect to the sampled area while in the second case, the Fourier transform was defined with respect to the entire illuminated aperture.

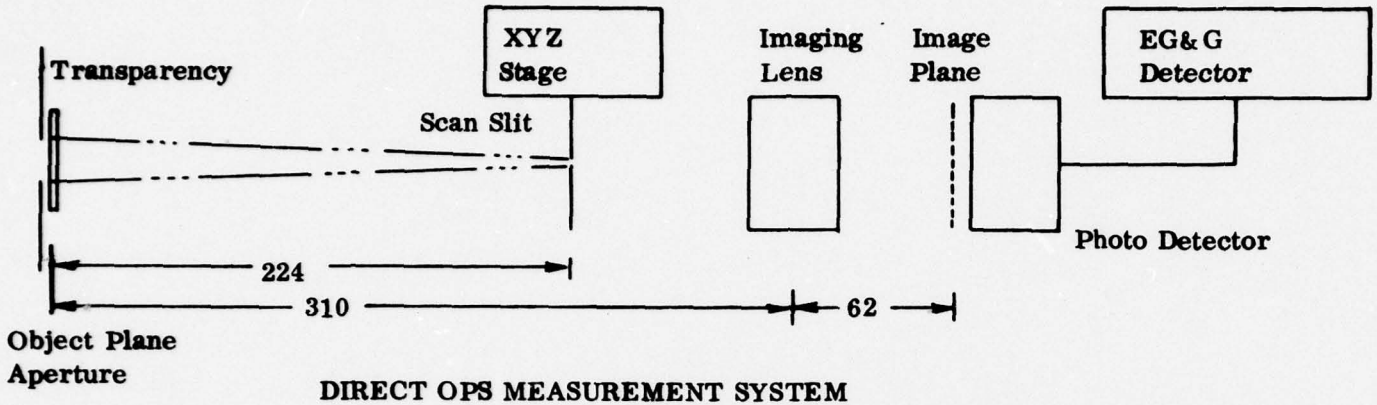

DIRECT OPS MEASUREMENT SYSTEM

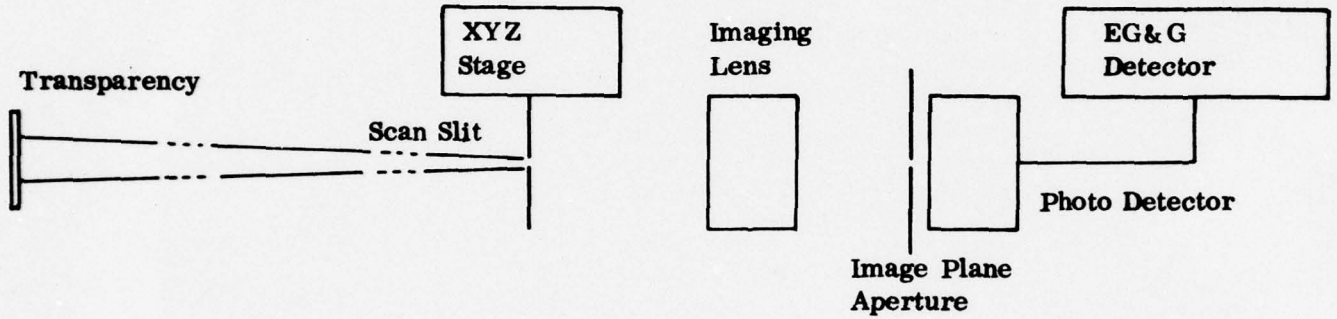

HOPS MEASUREMENT SYSTEM

Figure 3-8. Measurement Configurations for Direct OPS and HOPS Measurement Systems

TEST NO. 2 In this test the viability of placing an analog spatial filter that permits direct processing of OPS data is evaluated. In many OPS analysis applications, a linear weighting function (with maximum weighting at the center) is used for reducing the OPS measured data (e.g., a first moment weighting). This can be accomplished during the measurement process using optical analog processing. In this test a linear density wedge was used to obtain linear weighting of the measured OPS data. For demonstrating the concept, a tribar target was used as the input transparency. First a 5 mm aperture was used to isolate a single tribar at the plane of the transparency. The configuration was the same as in Figure 3-8. The optical power spectrum was sampled with the slit at intervals equal to the width of the slit. Secondly the slit was replaced by a linear density wedge with the maximum density at the d.c. of the spectrum. A rectangular aperture was placed over the linear wedge to expose only the area covered by the scanning slit (one half plane only). The light transmitted by the linear wedge was measured using the photometer. In the third case the 5 mm aperture in the transparency plane was removed and 1 mm aperture was placed in the image plane so as to simulate the HOPS measurement configuration. The linear wedge then spatially filters the input transparency and the 1 mm aperture samples the intensity image obtained. The photometer was once again used to read the sampled intensity. Using the transmission values of the linear density wedge and the scanned OPS data from the first measurement, the linear weighted average was calculated. The result was:

a. The calculated linear weighted average reading equals 0.186 units.

b. Measured weighted average using the conventional OPS measurement configuration equals 0.185.

c. Measured weighted average using the HOPS measurement configuration equals 0.199.

Part of the increase in the measured value for the third case can be attributed to the increased background scattering resulting from increased area of illumination

on the plane of the input transparency. However, a portion of the difference must also be due to the differences in the measurement systems.

TEST NO. 3 A major problem associated with the Reticon two-dimensional array prohibited its use in this HOPS measurement. When the portions of the detector array are saturated, the electronics associated with the Reticon array lost synchronization of the data scan. This resulted in meaningless data. It was impossible to use the detector array to obtain any quantitative data. This was not anticipated during the initial design phase of this equipment.

In this series of experiments, the camera back replaced the photometer and the spatially filtered intensity image was recorded under varying positions and shapes of spatial filtering masks. In the first case a fifteen bar target representing a one-dimensional image distribution was used as the input transparency. The spatial filter was the slit used in the quantitative measurements described above. The spatially filtered intensity image was recorded for various positions of the slit as it was moved away from the d.c. of the power spectrum. Figures 3-9 and 3-10 show examples of recorded imagery. Figure 3-9 using a 15 bar Diffraction Limited resolution target, clearly demonstrates the definition of the apertures associated with the various frequency groups.

As the higher frequencies are sampled, the filtered target image shows its respective high frequency image components. It is shown by this illustration that the HOPS record of the spatial image is also a record of the OPS contribution to each image area. For a continuous tone image, the HOPS output is given in Figure 3-10. In this case, an aerial photograph was used as the input transparency and a series of annualar masks were used in the frequency plane. Different features of clouds, streets, etc. are detected in the various filtered images. The artifacts in Figure 3-10 also show ringing caused by the hard clipping frequency filter. This is also known as Gibbs phenomenon.

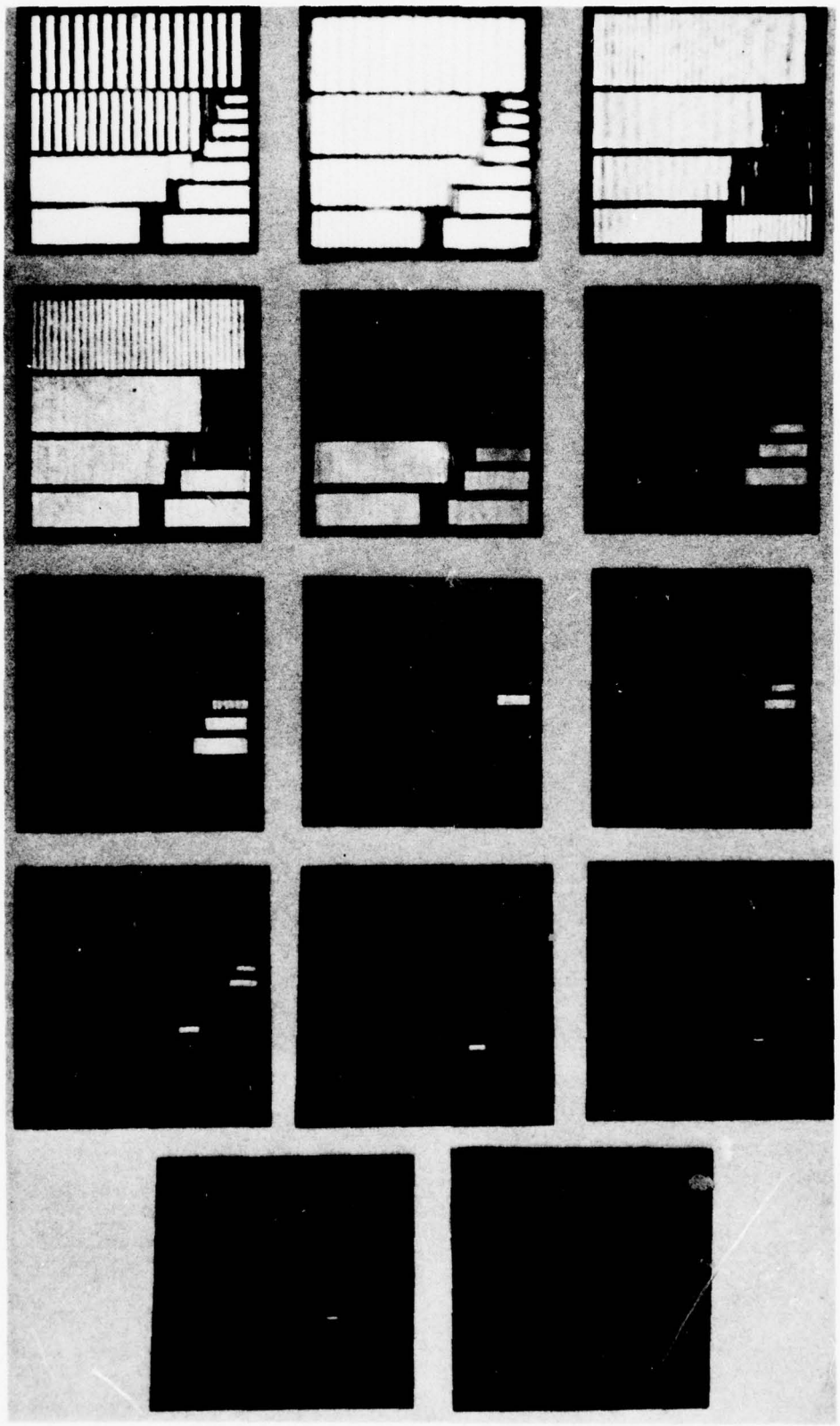

Figure 3-9 Visual Illustration of the HOPS Measurement Concept Using 15-Bar Target

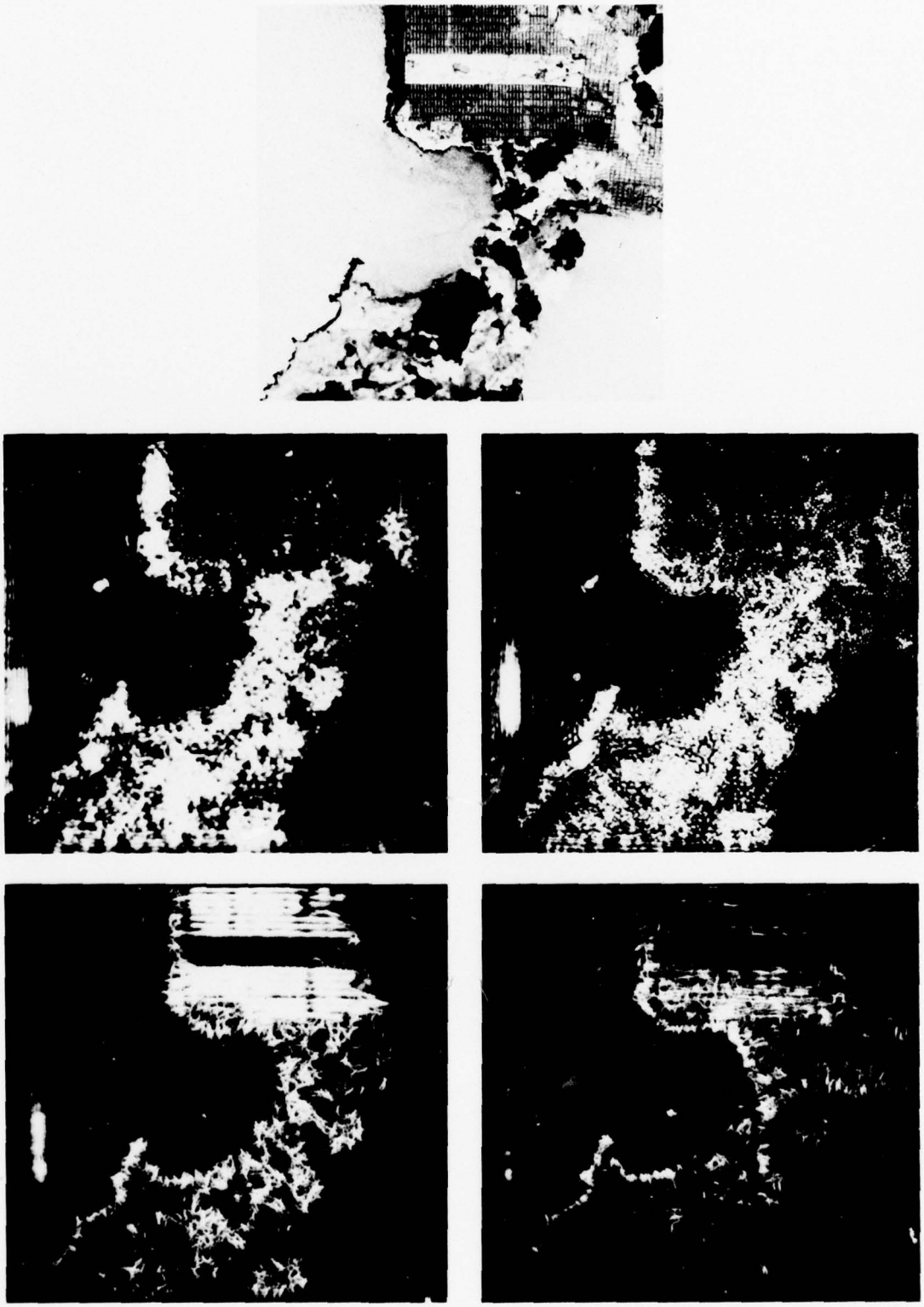

Figure 3-10. Examples of Spatially Filtered Intensity Images

TEST NO. 4 In this test we demonstrate use of a 100:1 dynamic range (D. R.) photodiode in a 10^4:1 D. R. HOPS measurement. The test target illustrated in Figure 3-9 was the input transparency. An image area of 1. 5 mm x 1. 5 mm, passing target elements of 10 to 100 ℓ/mm, was sampled with a United Detector Technology detector. The detector monitored the output image, and annular spectral masks were placed in the frequency plane. The detector was used in two modes, a full scale mode and a single scale mode limited to a 100:1 D. R. The measured data is plotted in Figure 3-11, where the solid line curve is the full scale measure of the sampled area. The dashed line curve was measured with the 100:1 D. R. sensor using ND filters to constrain the spectrum in a calibrated manner. This demonstrates that a large dynamic range signal can be measured using a smaller dynamic range detector by expeditious use of ND filters in the masks.

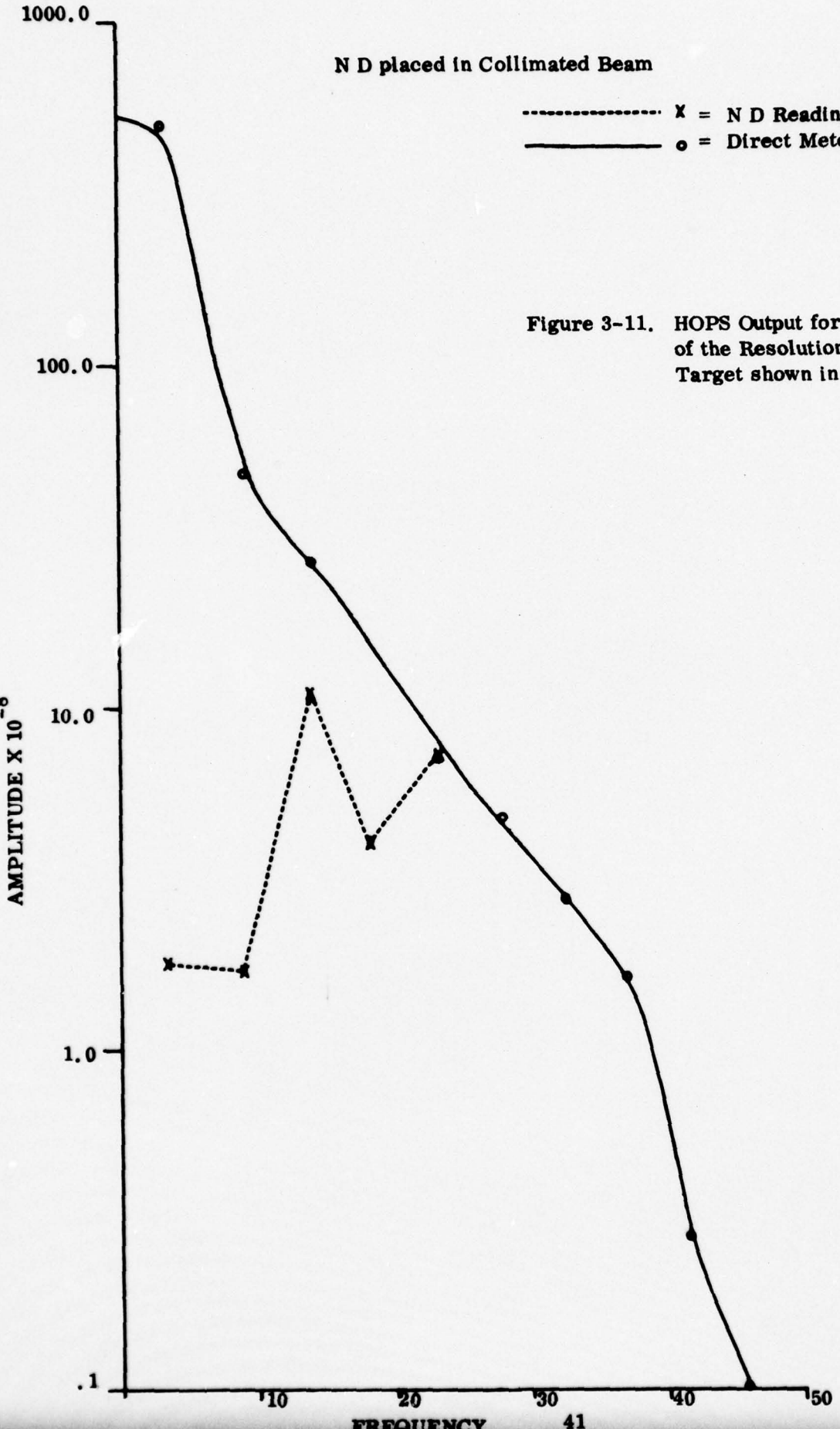

Figure 3-11. HOPS Output for Element of the Resolution Test Target shown in Figure 3-9.

4. RECOMMENDED HOPS DESIGN APPROACH

In this chapter we discuss practical design considerations of the HOPS. This analysis and discussion is presented to demonstrate the feasibility of the system design and its potential utility for high speed measurements.

4.1 Linear Detector HOPS Approach

A HOPS concept that appears most practical and avoids the pitfalls experienced with the two-dimensional matrix array, uses a linear photodiode array with parallel optics. This approach provides high scanning rates with uncomplicated hardware. The parallel optical HOPS approach is illustrated in Figure 3-2(b). Each optical channel contains a lens, spectrum sampling mask and a linear photodiode array. All channels are similar except for the mask that enables specific sampling of the input spectra. The number of channels is equal to the number of masks required for the spectrum sample. For a "one-shot" analog mask, only one channel is required. In this system the film is continuously moving through the entrance aperture and scanning is performed by the self-scanned photodiode arrays with no mechanical or optical scanners required. The geometry for film sampling, as specified by the Customer, requires 40 samples across a 9 inch film width to yield an effective sampling aperture of about 0.225 inches. As noted below, this is not a stringent requirement for an electro-optical detection system. An analysis of the system is given here.

As a starting point, we consider the linear photodiode array. Until now users of solid state image sensors have had to choose between devices optimized for low-noise readout (CCD arrays) and devices with optimized sensor characteristics (photodiode arrays). The advantages of both devices have been obtained in a new family of image sensors, the CCPD (Charge Coupled Photodiode) arrays. The CCPD utilizes photodiode sensors with CCD readout registers and output buffer amplifiers for low noise signal extraction.

CCPD devices are presently available with 256 and more sensor elements. For the HOPS design we require only 40 elements. This can be obtained by integrating the 256 array over a number of element subsets to obtain a 40 element sensor. However, we expect that Reticon will expand the CCPD line to other photodiode array designs presently available, such as the RL64A array. This array has 64 elements on 2 mil centers, with 2x2 mil element areas. For the system analysis given below we use the geometry of the RL64A with CCPD response characteristics to predict expected HOPS capability.

The CCPD has the performance characteristics described in Table 4-1. This array has unique advantages in dynamic range, with better than 1000:1 expected in practice. In addition the array has special saturation anti-blooming gates. Saturation of one element does not delete array response as was experienced with the matrix array (Section 3.5.3).

TABLE 4-1

LINEAR ARRAY PERFORMANCE CHARACTERISTICS

Dynamic Range	
Peak to peak	500
rms	2500
Saturation Exposure	0.5 $\mu s/cm^2$
Responsivity	2 $V/\mu s/cm^2$
Average dark signal	10 mV
Saturation Voltage	1 mV
Peak to Peak noise	2 mV
RMS noise	0.4 mV (approx.)

4.2 Optical Scale

The linear array is positioned such that a 9" film is contained within the array format. The array is 0.128" long, requiring an optical reduction of 0.014, or 70.3:1 scale change from input to detector plane. This is a reasonable optical scale for which commercially available lenses can be purchased. At this scale, the array samples a 9" x 0.14" film area.

The HOPS linear detector can also be fabricated from discrete photodiodes. Sizes from 1 mm square to 1 cm square are available. Since only 40 elements are required, the diodes can be aligned and sampling and scanning electronics designed for the desired HOPS response characteristics. Thus, we are not constrained to a commercially available linear photodiode array.

4.3 Film Slew Rates

The film scanning requirements supplied by the Customer are the following:

9" film width
1/4" film sampling aperture
2 sec/frame (40x40 samples/frame)
1 OPS sample/ms (sample decision)

If we transfer these specifications to the geometry of an available linear array, the required number of line scans per 9" frame length is 64. At the desired scan period of 2 sec/frame (4.5"/sec film slew rate), the array scan rate must be 2.1 kHz (4.5"/sec x line/0.14" x 64 samples/line equals 2057 samples/sec). The CCPD can operate up to 5 MHz scan rate. If a film slew rate of 100 ft/min is desired, the array scan rate remains less than 10 kHz. The CCPD linear array scan rate is, therefore, not a limiting factor in HOPS design considerations.

4.4 Illumination Requirements

The sensitivity of the CCPD linear array is $2V/\mu s/cm^2$. The integration time of a CCPD element is selected by system design parameters. If we use Customer specifications listed in Section 4.3, a 4.5"/sec film slew rate specifies a diode element integration time of 3.1 ms.

The power density (irradiance) in the detector plane for saturation is:

- Saturation exposure — $0.5\ \mu s/cm^2$
- Integration time — 3.1 ms
- Power density for saturation — $167\ \mu w/cm^2$

To determine source requirements for a HOPS design with the CCPD array sensor, we must evaluate the energy level transmitted through the spectral masks. We use an OPS sample to determine this. The OPS distribution for an industrial scene is given in Figure 4-1. This shows relative energy measurements through 20 annuli for two-dimensional and one-dimensional OPS samples. The one-dimensional sample uses a slit aperture over the annuli to obtain a small angular sample of the spectrum. As noted from this distribution, the OPS dynamic range is approximately 3.5 and 5 decades for the 2D and 1D spectrum measurements, respectively.

Normalization of the energy through the annular bands can be effected with ND filters, reducing the OPS D.R. that must be sensed. For example, an ND 2.0 filter at band 1 provides approximate equalization of band 1 with band 3. Calibration enables accurate control of normalizing filters to reduce OPS D.R. to desired levels. Figure 4-2 gives a plot of density filters versus bands to approximately normalize the 2D OPS distribution to a constant, set at the band # 20 value. By this means the dynamic range to the detector is effectively reduced to that of the input transparency.

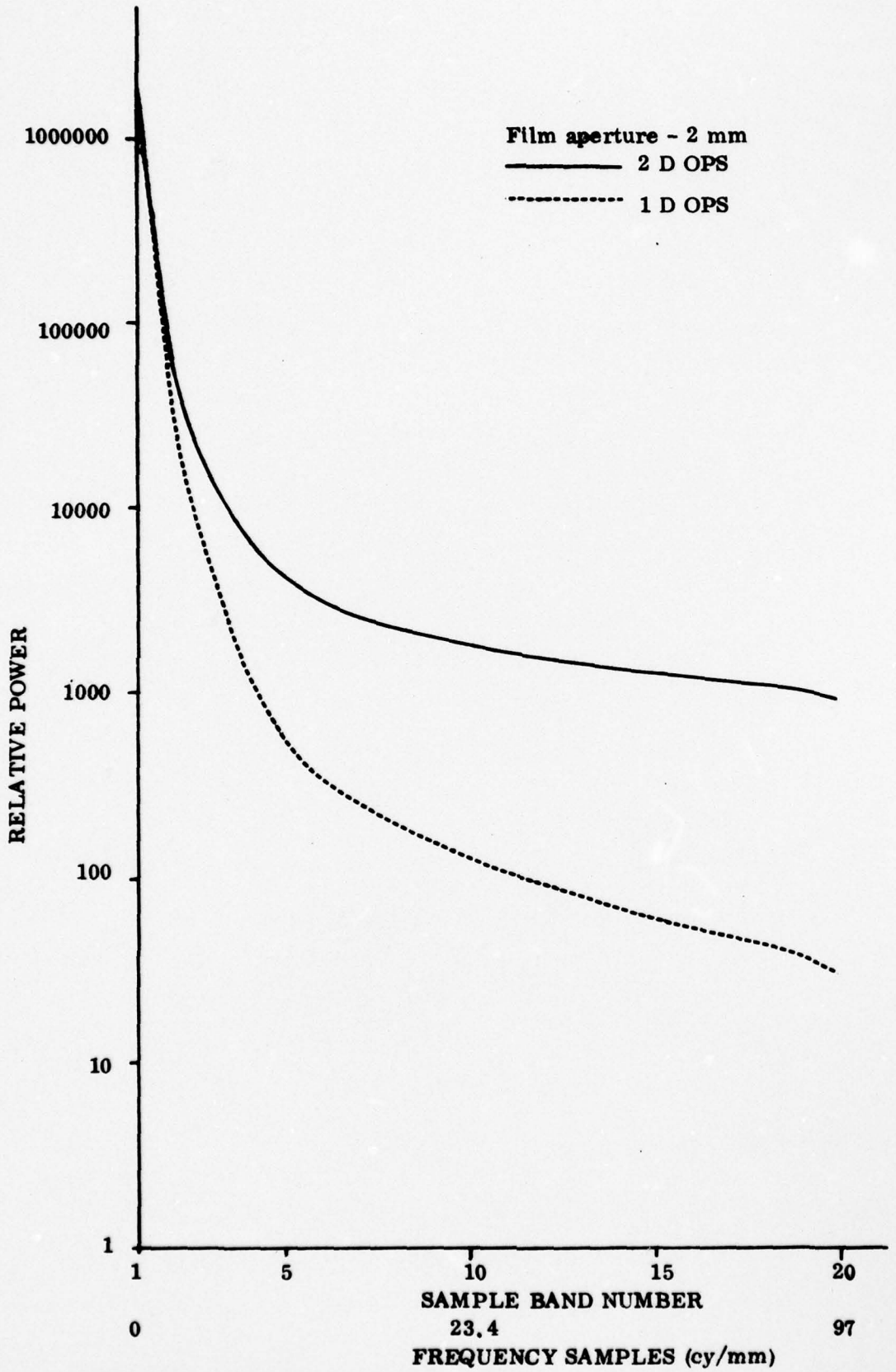

Figure 4-1. OPS Sample of an Industrial Scene Taken with the EIKONIX Series 5001 Power Spectrum Analyzer.

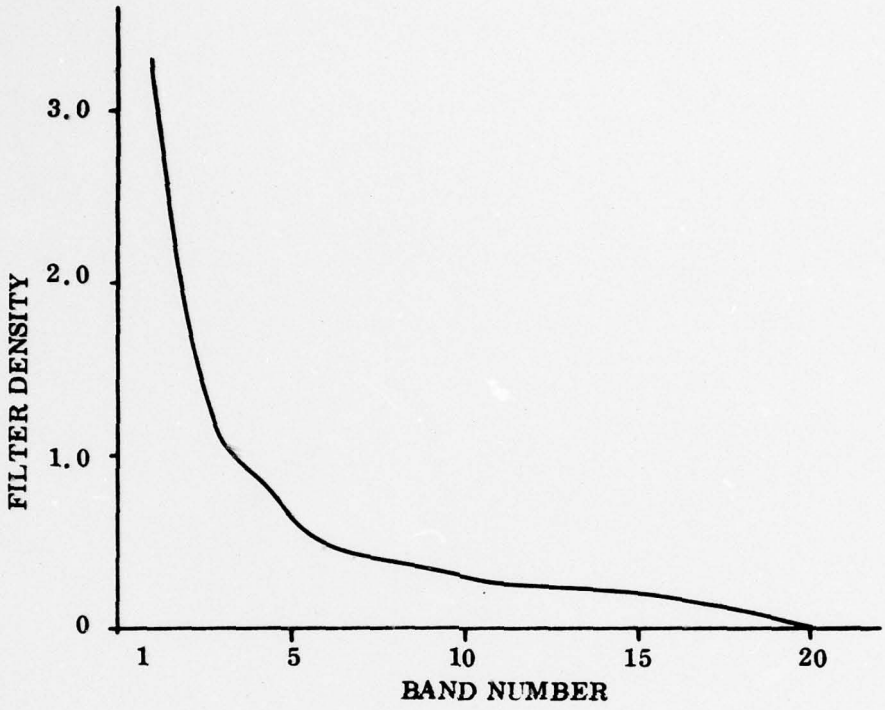

Figure 4-2. Transmission Filter Versus OPS Sample Bands for Reduction of Detector Dynamic Range Requirements

The source power required for this system is computed from the following parameters:

• power at detector for saturation at 3.1 ms integration time (p. 45)	167 $\mu w/cm^2$
• elemental area sampled on film (p. 44)	0.126 cm^2
• estimated optical transmission of imaging optics	0.80
• estimated transmission of laser filter-collimator	0.50
• spectrum mask transmission with 2D normalizing filter	0.01

- total power of source/ element area at 70.3 scale — 1.1 μm
- estimated source energy to illuminate a rectangular film area, 5 mm x 250 mm — 0.1 mw

Source requirements for the HOPS design are, therefore, relatively moderate.

4.5 Dynamic Range

The dynamic range of the HOPS system is at most 10^5 for the 1D measure and 10^3 for the 2D measure. Another 10^2 is expected from film transmittance. The CCPD detector dynamic range is 10^3. An additional 10^2 can be gained by variable integration time of the diodes. Integration time is clocked separately from scan time and can be decreased from the maximum 3.1 ms by more than a factor of 100. Thus, a detection range of 10^5, sufficient for the 2D OPS application, can be obtained from the detector. Additional range is obtained from ND filters in the optical channels as described above. With ND 2.0 filters, the HOPS dynamic range becomes 10^7, exceeding the requirement of even the 1D OPS D.R.

4.6 Optical Design Considerations

The basic optical configuration of the HOPS system is simple and cursory examination would indicate that there is considerable flexibility in choosing the system parameters. However, there are some constraints on the options available in choosing the various parameters for the HOPS system. For the purpose of this analysis the optical configuration illustrated in Figure 4-3 is used. It is assumed that the entrance pupil of the imaging lens is in coincidence with the spatial filter plane.

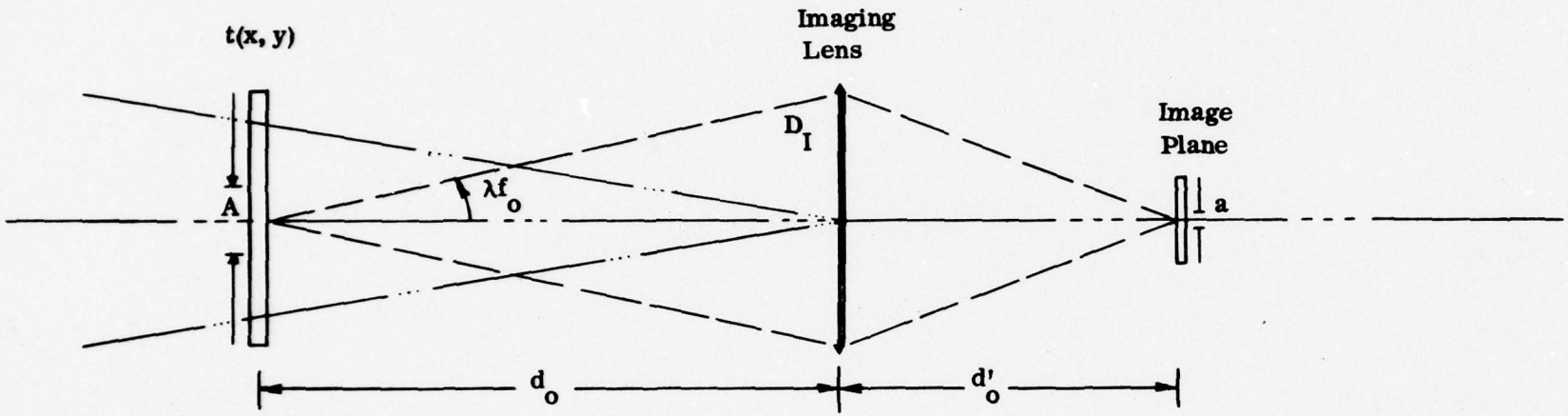

Figure 4-3. . Transforming and Imaging Optics

If f_0 is the maximum spatial frequency of interest, the entrance pupil diameter of the imaging lens must be

$$D_I = 2\lambda f_0 d_0 \tag{4.1}$$

where λ is the wavelength of light and d_0 is the distance illustrated in Figure 4-3. If $F_I\#$ is the f-number of the imaging cone

$$F_I\# = \frac{d_0'}{D_I} \tag{4.2}$$

where d_0' is the imaging distance. Hence,

$$d_0' = 2\lambda f_0 d_0 F_I\# \tag{4.3}$$

The magnification of the imaging lens M is given by

$$M = \frac{d_0'}{d_0}$$

Therefore,

$$M = 2\lambda f_0 F_I\# \tag{4.4}$$

If A is the aperture diameter at the transparency plane and a is the lateral extent of the detector aperture in the image plane,

$$a = 2\lambda \phi \cdot F_I\# \tag{4.5}$$

where $\phi = A f_0$ is the space bandwidth product.

If we assume $\lambda = 0.5$ microns and if a is expressed in microns, the maximum spatial-bandwidth product that can be measured using HOPS configuration is given by

$$\phi = \frac{a}{F_I\#} \tag{4.6}$$

Practical imaging considerations limit the imaging cone f-number to be no less than a value of 2. Hence,

$$a = 2\,\phi \tag{4.7}$$

There are two design considerations to consider. One is the space bandwidth capability of the lens, as defined by the requirement ϕ. The second is the transparency sampling requirement as defined by HOPS design objectives. The first can be estimated from 9 inch film with a desired detectable frequency limit of 50 cy/mm. Then ϕ is 11,430, that denotes an image plane sampling array size of 22.86 mm from equation (4.7). The second design consideration specifies at least forty samples across the film array, that is $a = a'n$, defining each element size a minimum of 0.57 mm. Thus, a discrete diode array having element size of .57 mm or greater satisfies the requirements of HOPS.

During the initial investigation of HOPS measurement, it was proposed to optically translate laterally the power spectral distribution within the entrance pupil of the imaging lens. This would permit incorporation of a two-dimensional array of spatial filtering masks in the transform plane. The system design would not be concerned with the mechanical problems associated with replacement of spatial filtering masks as they would be optically addressed. The proposed system is shown in Figure 4-4. The lateral displacement of the power spectrum within the

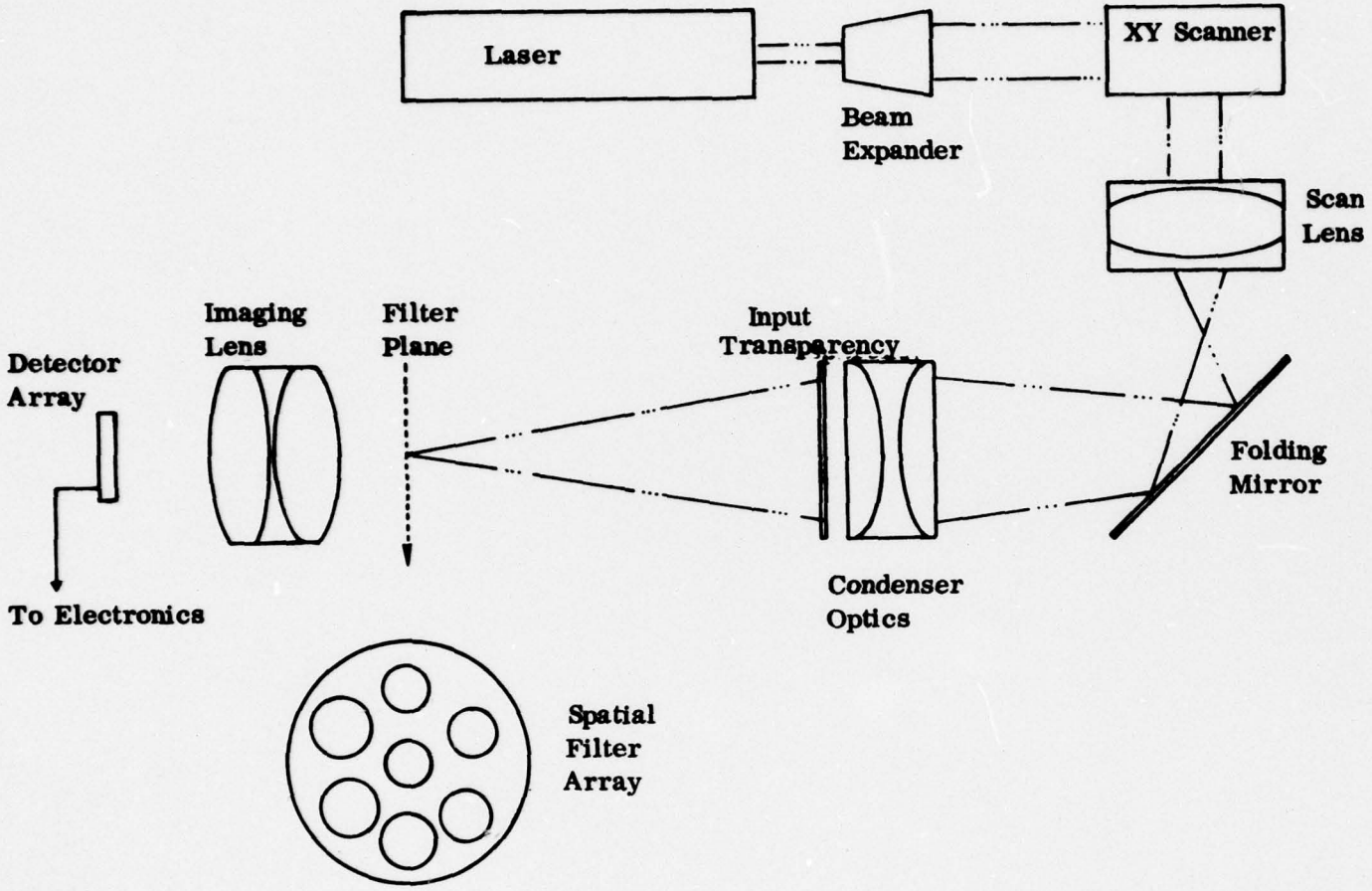

Figure 4-4. HOPS System with Filter Array in Lens Aperture

entrance pupil can be accomplished using an XY laser scanner. Because of the independence of the transform and the imaging optics, there is no displacement of the final image with respect to the diode array.

The problems associated with the implementation of this concept become clear in light of the above analysis. If the entrance pupil has to be divided by several spatial filtering masks, then there has to be a corresponding reduction in the space-bandwidth product that can be utilized. This approach to addressing filter masks is impractical.

Another consideration is the HOPS flare level due to the optics. The point spread function of a lens can introduce cross-talk between detector elements and impose the dynamic range threshold of the system. An OPS lens evaluated at EIKONIX has a flare threshold shown in Figure 4-5 for on-axis and off-axis operation. In image space the dynamic range required is that due to the transparency (10^2) and that due to the spectrum differences (10) after ND normalization. At the 10^3 level, the noted lens has 0^o spread function diameter of approximately 88 μm. This is a small fraction of the detector size, and should have a negligible impact in HOPS detection.

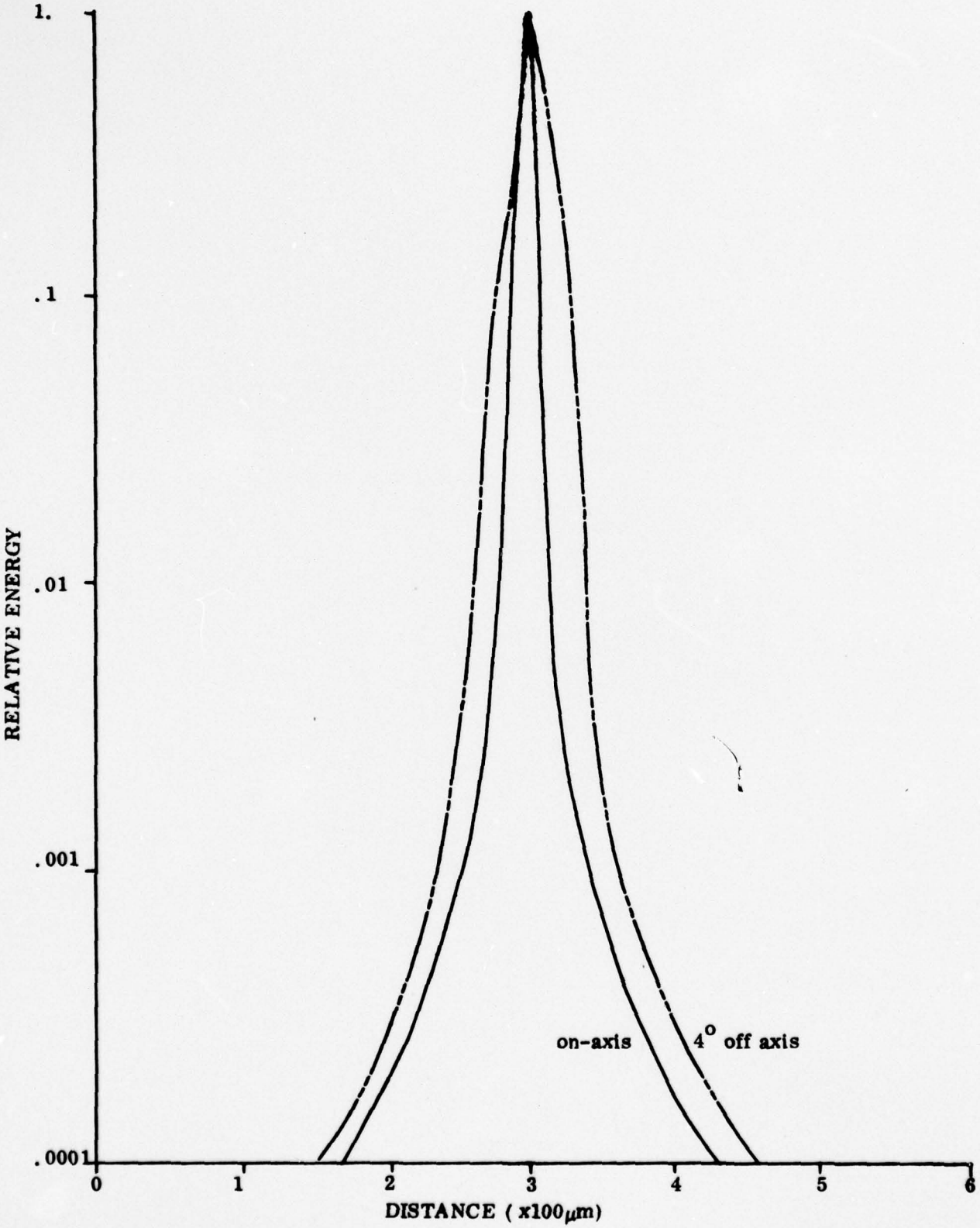

Figure 4-5. Point Spread Function of a 210 mm Voigtlander Heliar, f/4.5 lens, on axis and 4° off axis.

5. CONCLUSIONS AND RECOMMENDATIONS

5.1 Introduction

In this investigation a different approach to OPS measurement has been proposed and its preliminary feasibility has been evaluated. The motivation was to investigate a system that would have potential advantages in the application of optical power spectrum measurement techniques to feature extraction problems in mapping.

5.2 Conclusions

The theoretical and experimental analyses conducted during the period of this investigation support the following conclusions:

a. The HOPS measurement concept differs from conventional OPS measurement systems but still permits OPS measurement and definition of input transparency sample elements for feature extraction applications.

b. The theoretical and experimental results show that the HOPS measurement scheme is feasible. From an optical and system configuration point of view, HOPS provides an attractive alternative to large format OPS systems involving laser scanners. The potential advantages of the HOPS system in terms of increased speed and operational flexibility should be demonstrated using a one-dimensional array.

c. The commercially available two-dimensional detector arrays are not suitable as image plane detectors because of their electro-optical characteristics. The two-dimensional arrays cannot operate under conditions where detector elements are saturated. This problem does not exist with one-dimensional arrays, that have been tested.

d. The possibility of utilizing an array of spatial filters within the entrance pupil of the imaging optical systems as a means of overcoming the mechanical problems associated with interchanging spatial filtering masks is not practical due to the undue demands it imposes on the F# requirements of the imaging lens system.

e. Analysis of the HOPS design demonstrates that the one-dimensional detector design is practical from the point of view of quality requirements of commercial lenses, light sources and detectors. The detector element size must be .57 mm or larger.

5.3 Recommendation

On the basis of the results of this program the following recommendation is made:

The HOPS design should be evaluated in an experimental applications program. The design should use a one-dimensional detector array. The measurement program should fully test the utility of spectral normalization with neutral density filters, and spatial and spectral discrimination in sampling over the required dynamic range. This system approach provides the most advantageous means for rapid OPS measurements. And this test will conclusively demonstrate the utility of HOPS in practical applications.

REFERENCES

1 A. Vander Lugt, "Coherent Optical Processing", Proceeding IEEE, Vol. 62, No. 10, pg. 1300 (1974)

2 B.J. Thompson, "Optical Data Processing", Optical Transforms by Lipson, Academic Press, N.Y. 1972

3 J.W. Goodman, "Introduction to Fourier Optics", Text, McGraw-Hill, New York 1968

4 E.L. O'Neill, "Spatial Filtering in Optics", IRE Trans. Information Theory, Vol. IT-2 June 1966

5 M. King et al, "Real Time Electro Optical Signal Processors with Coherent Detection", Applied Optics, Vol. 6, pg 1367, 1967

6 E.B. Felsteao, "A Simplified Optical Correlator", Applied Optics, Vol. 7, pg. 105, 1968

7 M. Gottleib et al, "Optoacoustic Processing of Large Time Bandwidth Signals", Applied Optics, Vol. 11, pg. 1068, 1972

8 M. Gottleib et al, "Design and Construction of an Optoacoustic Signal Processor", Applied Optics, Vol. 12, pg. 1922, 1973

9 D.L. Hecht, "Broad Band Acousto-Optics Spectrum Analysers", Ultra-Sonics Symposium, Nov. 1973

10 D.L. Hecht, "Acoustooptical Devices for Optical Information Processing up to 16Hz Bandwidth", JOSA, Vol. 67, pg. 1444, 1977

11 G.G. Lendaris and G.L. Stanley, "Diffraction Pattern Sampling for Automatic Pattern Recognition", Proc. IEEE, Vol. 58, pg. 198, Feb. 1970

12 N. Jensen, "High Speed Image Analysis Techniques", Photogrammetric Engineering, Vol. 39, pg. 1321, 1973

13 G.E. Lukes, "Cloud Screening from Aerial Photography", Proc. SPIE, Vol. 45, 1974.

REFERENCES (Continued)

14 R. D. Leighty and G. E. Lukes, "Cloud Screening from Aerial Photography, Proc. ASP, 40th. Annual Meeting, March 1974

15 Balasubramanian, N., "Optical Leverage Telecentric Scanner", Internal Memo, Center for Coherent Optics, U. S. Army Engineering Topographic Laboratories, Ft. Belvoir, Va. 22060

16 R. Bracewell, "The Fourier Transform and Its Applications", McGraw-Hill, 1965

17 S. B. Campana, "Techniques for Evaluating Change Coupled Imagers", Optical Engineering, Vol. 16, No. 3, 1977

APPENDIX A

SYSTEM DESIGN CONSIDERATIONS IN OPTICAL POWER SPECTRUM ANALYSIS

SYSTEM DESIGN CONSIDERATIONS IN OPTICAL POWER SPECTRUM ANALYSIS

N. Balasubramanian and H. J. Liff
EIKONIX Corporation
103 Terrace Hall Avenue, Burlington, Massachusetts 01803

Abstract

Although the optical power spectrum (OPS) is widely used in pattern recognition and image assessment application, relatively little literature exists on the practical design considerations for OPS systems. This paper addresses some of these relevant issues. We illustrate the three standard configurations for OPS systems but limit our detailed attention to only one. We establish a limit on the space bandwidth product for neglecting the curvature of the transform surface, devise formulae for the laser power requirements, and consider the effects of film substrate thickness and scan center stability on system performance. We conclude with brief remarks on the effects of spectral and temporal coherence.

Introduction

The use of optical power spectrum analysis for pattern recognition and image assessment has been demonstrated by several investigators (1-4). Custom configured OPS measurement systems are commercially available and are being applied to a variety of special applications (5, 6). While the theory and the potential capabilities of OPS analysis have been widely documented, there has been relatively little attention to the practical design considerations associated with OPS systems. The intent of this paper is to enumerate the various system parameters associated with OPS measurements and examine their effect on overall system performance.

We emphasize that in this paper consideration is given only to systems used to measure the power spectral distribution. A clear distinction must be made between these systems and the coherent optical processing systems used for linear filtering applications. Many of the fourier transform lens design considerations and system tolerance specifications documented in the literature (7-9) are not directly relevant to OPS systems; even though, the OPS systems rely on the fourier transform properties of lenses.

A detailed discussion of the design considerations of each and every component comprising the OPS system is beyond the scope of this paper. Hence, consideration is given only to a few of the system components and numerical examples are presented to emphasize their significance.

Basic System Description

A basic system configuration for an OPS measurement system is illustrated in Figure 1. The system components can be classified into five groups. They are:

1. The source.
2. Sample aperture forming optics.
3. The input transparency.
4. The transform optics.
5. OPS sampling detector.

There are several design parameters associated with each of the component groups. These are listed in Table I. The optimum combination of the design parameters for each of the component groups depends on the intended application. A close examination of the parameters listed in Table 1 reveals the complexity associated with OPS measurement systems. The overall system performance depends upon the interaction between the parameters associated with each component. It is the objective of this paper to outline the considerations necessary for choosing the design parameters.

System Configurations

Three possible configurations for producing the power spectral distribution are shown in Figure 2. In each case the input illumination is collimated, monochromatic light and the amplitude distribution produced in the back focal plane is related to the two-dimensional fourier transform of the input transparency. In the first case, the input transparency is placed at the front focal plane of the lens. In the second case, the transparency is placed close to the entrance aperture of the lens. In the third case, it is placed behind the lens at a given distance, d_o, from the back focal plane.

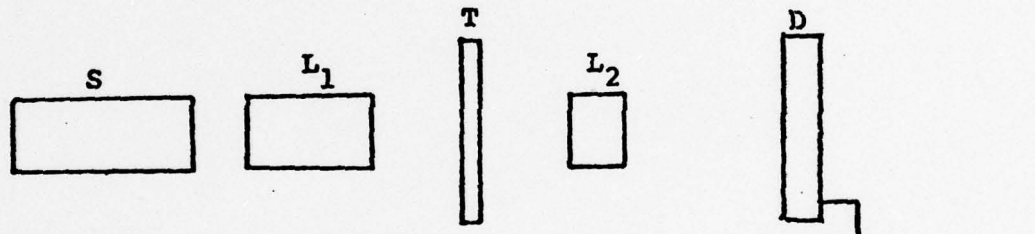

S ... SOURCE
L_1... SAMPLE APERTURE FORMING OPTICS
T ... TRANSPARANCY
L_2... TRANSFORM OPTICS
D ... OPS SAMPLING DETECTOR

Figure A-1 Basic System Description

TABLE 1

COMPONENT	DESIGN PARAMETER
1. Source	a. Power output b. Power stability c. Spatial coherence d. Temporal coherence
2. Sample Aperture Forming Optics	a. Size b. F- Number c. Wavefront distortion d. Intensity distribution e. Laser power coupling efficiency
3. Input Transparancy	a. Substrate optical quality b. Substrate thickness c. Mean density d. Power spectral dynamic range e. Phase effects and noise
4. Transform Optics	a. Size b. F- Number c. On and off axis aberrations
5. OPS Sampling detector	a. Spatial frequency bandwidth b. Size c. Dynmic range d. Sampling rate

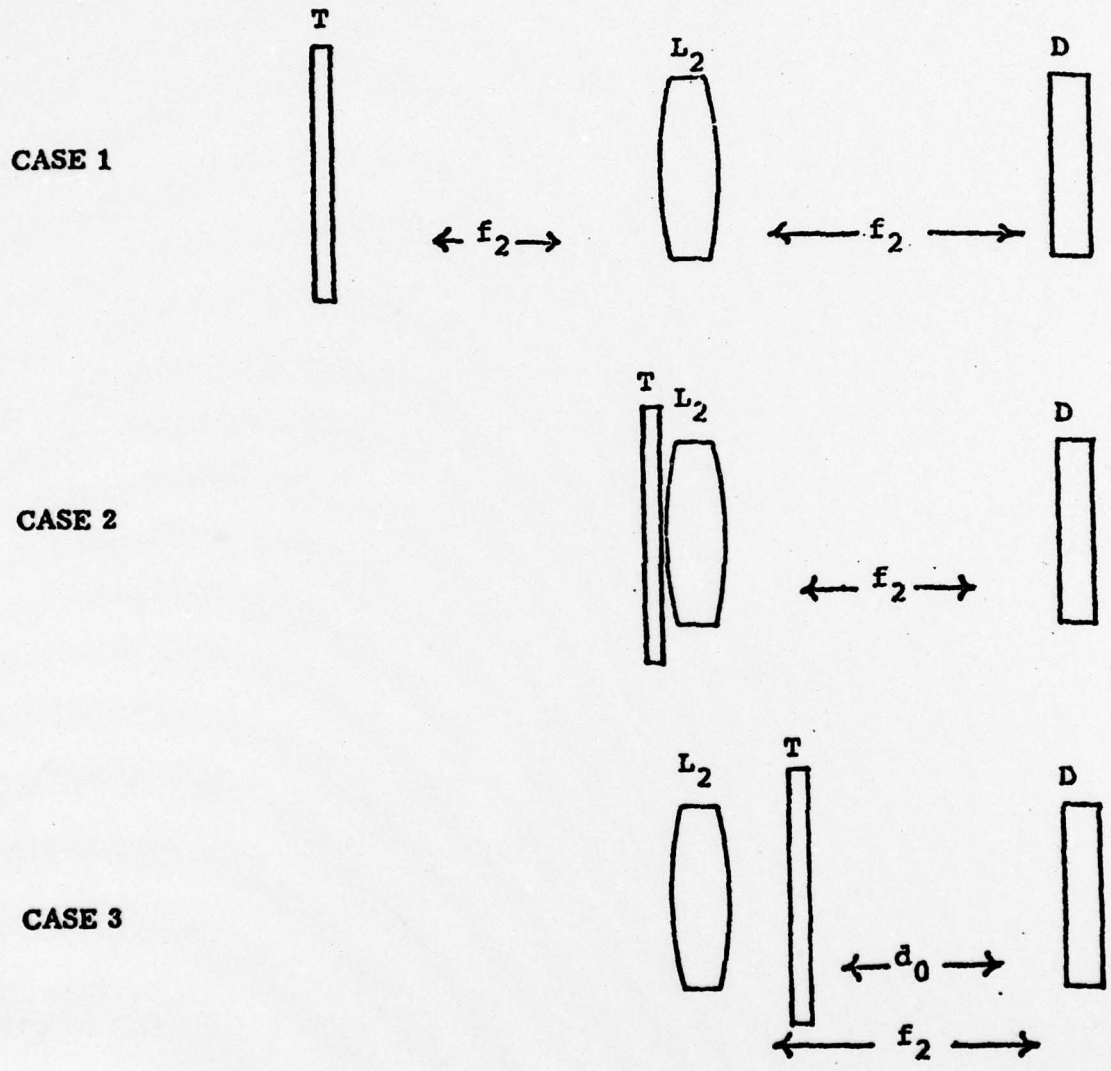

Figure A-2 System Configuration

For OPS measurements it is the intensity in the back focal plane which is of concern, hence the different "phase factors" associated with each of the three systems is of no concern. (10) From a theoretical point of view, the systems are identical. However, the optical requirements on the transform lens are different in each case.

Consider the requirements for a sampling aperture of diameter a_T and a maximum spatial frequency of interest F_o. For case 1 the aperture of the lens is given by

$$a_2 = 2\lambda F_o f_2 + a_T$$

where f_2 is the focal length of the lens and λ is the wavelength. The half field angle over which the lens must be diffraction limited is therefore

$$U_{p2} = \lambda F_o.$$

For case 2

$$a_2 = a_T$$

and the field angle requirements are the same as for case 1.

The diameter of the transform lens for case 3 is

$$a_2 = \frac{f_2}{d_o} a_T$$

and there are no off axis optical requirements necessary for the transform lens. The transform lens need be diffraction limited only for an on axis monochromatic collimated beam. An additional advantage of case 3 is that the scale of the power spectral distribution can be changed by varying d_o. The linear displacement, x_D, in the back focal plane is related to the spatial frequency F by

$$x_D = \lambda F d_o.$$

These first order design considerations indicate that the system configuration shown in case 3 has advantages over others in the application to OPS measurement. The analysis presented in this paper shows the limits of applicability of this system configuration. All other system considerations are also presented with the context of the configuration shown in case 3.

In configuration shown in case 3, the power spectral distribution is actually formed on a spherical surface whose center of curvature is located at the intersection of the optical axis and the input transparency. When the distance between the input transparency and the focal point is large and if the diffraction angles considered are small, the spherical surface can be approximated by the back focal plane. It is easy to evaluate the domain of applicability of this approximation.

Considering Figure 3, the sag of the spherical surface is given by

$$s_1 = \frac{\lambda^2 F_o^2 d_o}{2}$$

where f_o is the maximum spatial frequency of interest, λ is the wavelength and d_o is the distance between the transparency and the focal point. For the spherical surface to be approximated by the focal plane, the sag of the spherical surface must be smaller than the depth of focus of the converging beam. Hence

$$s_1 < \Delta F_2$$

where ΔF_2 is the depth of focus given by

$$\Delta F_2 = \lambda (f_2^{\#})^2$$

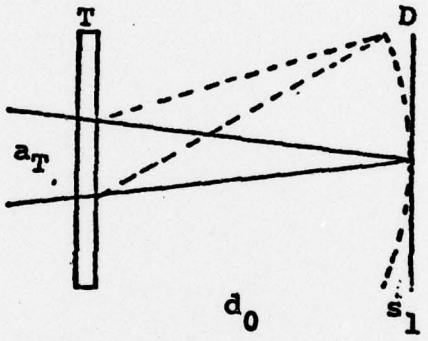

Figure A-3 Power Spectral Surface Curvature Effects

where $f_2^{\#}$ is the F-number of the converging beam.

$$\Delta F_2 = \lambda\left(\frac{d_o}{a_T}\right)^2$$

where a_T is the sample aperture. Hence

$$\frac{\lambda^2 F_o^2 d_o^2}{2} < \lambda\left(\frac{d_o}{a_T}\right)^2$$

or

$$(F_o a_T)^2 < \frac{2 d_o}{\lambda}$$

$$F_o a_T = \Phi < \sqrt{\frac{2do}{\lambda}}$$

where Φ is the space bandwidth product on the transparency. Example

$$d_o = 200\text{mm}$$
$$\lambda = .5 \times 10^{-3}\ \text{mm}$$

$$\Phi_{max} = 900.$$

This means that if the sample aperture is 10mm, the maximum spatial frequency for which the approximation is valid, is about 90 lines per mm.

Analysis of System Parameters

A complete analysis of the various parameters associated with each component and the determination of the optimum combination based on specific system requirements are beyond the scope of this paper. However, analysis is presented here to demonstrate the methodology in the definition of the various component parameters. The analyses presented in this section relate to:

a) Laser power requirements.

b) Optical system considerations.

c) Coherence effects.

Laser Power Requirements

The laser power required depends on various system parameters including the transmission of the optical components, the average transmission of the transparency, the dynamic range of the power spectral distribution, the sensitivity of the detector and the required signal to noise ratio. In this section the laser power requirement is examined from the point of view of the detector characteristics and the dynamic range of the power spectral distribution

The two different detector systems that are considered are illustrated in Figure 4. The first detector consists of a series of annular segments placed in the spectral plane. Each annular segment measures the power contained within a frequency band ΔF defined by the width of the segment. The radius corresponding to the center of the annulus defines the spatial frequency, F, at the center of the band. The second detector system consists of an annular mask and a condensing lens used to pass the power spectral distribution onto a single detector. The details of the detector systems discussed are illustrated in Figure 4.

Detectors are commonly characterized by their specific detectivity D* defined by

$$D^* = (A_d/T_s)^{1/2}\,(S/N)\,(1/P) \qquad (1)$$

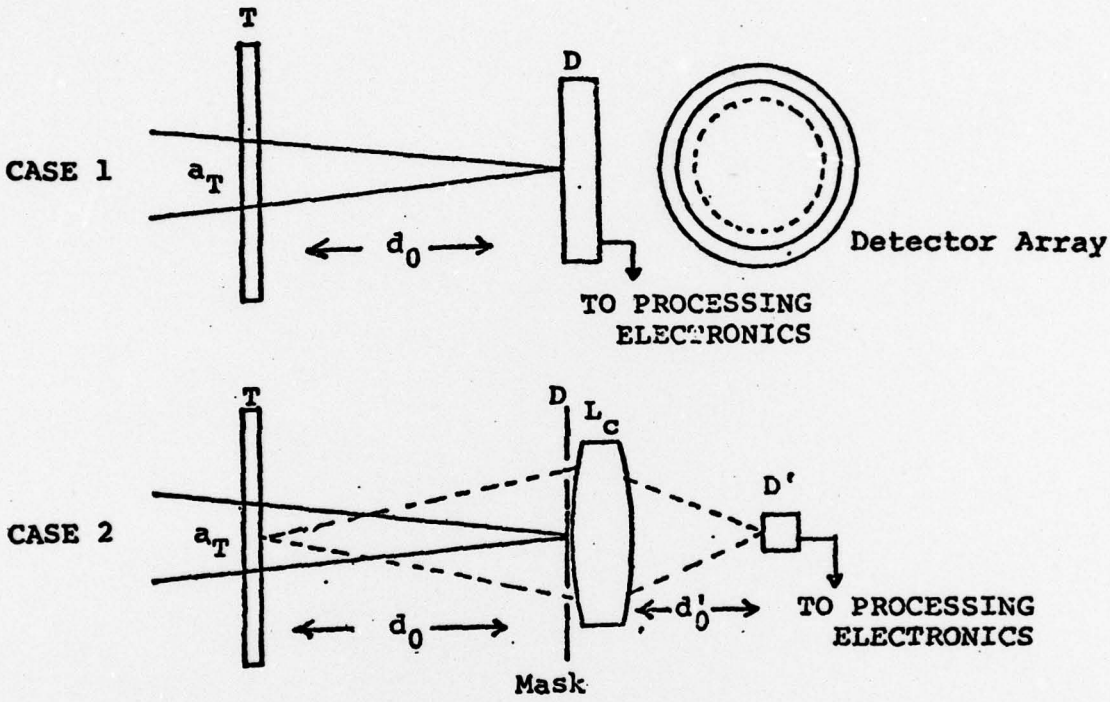

Figure A-4 Detector System Configuration

where

A_d = detector area

T_s = sampling time

(S/N)=signal to noise ratio

P = power incident on the detector.

For the annular detector

$$A_d = 2\pi (\lambda d_o)^2 \; F\Delta F.$$

If P_L is the laser power, T_o the transmission of the optics, and T_t, the average intensity transmission of the transparency then the power incident on the detector can be written as

$$P = P_L T_o T_t / D_F$$

where D_F is a dynamic range factor which depends upon the characteristics of the transparency and defines the fraction of power diffracted into a given band.

From the above definition, it follows that

$$D^* = 2\sqrt{\pi} X_D (1/RT_s)^{1/2} \; (S/N) D_F / P_L T_o T_t \qquad (2)$$

where

$$X_D = \lambda d_o F_o, \; R = \frac{\Delta F}{F_o}.$$

X_D is the radius of the largest annulus and R is the number of annular segments. If we let $B = 1/RT_s$ represent the number of complete power spectral measurements made per second, the required laser power is given by

$$P_L = \sqrt{2\pi} X_D (B)^{1/2} (S/N) (D_F / T_o T_t) \; 1/D^*. \qquad (3)$$

As an example let

X_D = 1.5 cm

B = 1600

(S/N)= 50

$D_F = 10^4$

$T_o T_t = 0.05$

$D^* = 10^{12}$

then

$P_L = 3 \times 10^{-3}$ watts.

Figure 5 shows a plot of the power requirement against $\sqrt{B}$ for various values of D_F.

Balasubramanian, Cliff

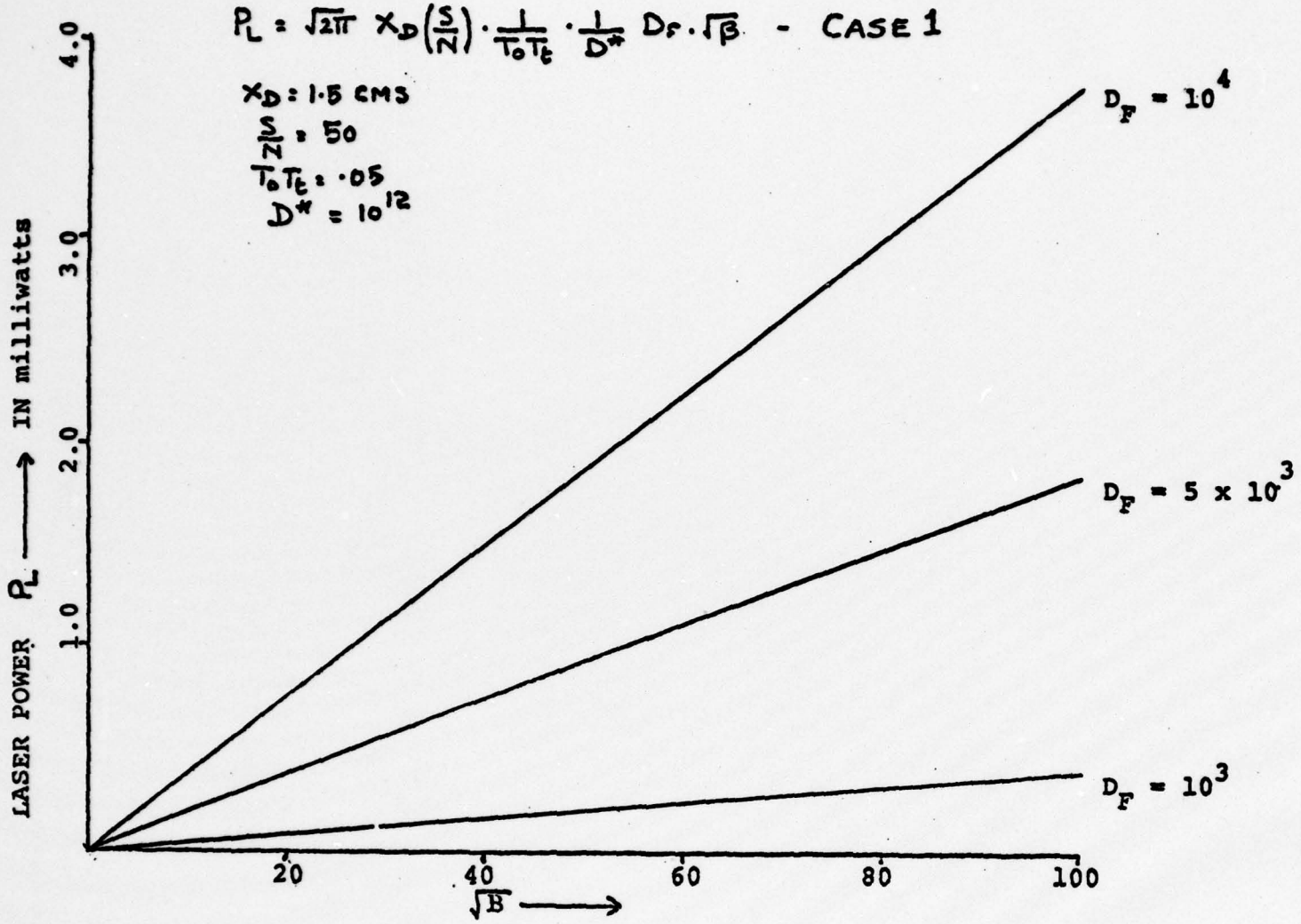

FIGURE A-5 Laser power as a function of data rate.

To consider the second detector of Figure 4, we shall assume a minimum detector size which can be achieved if the condensing system images the sample aperture onto the detector. The diameter of the detector is then given by

$$a'_D = a_T \frac{d'_o}{d_o}$$

where d'_o is the distance between the condenser lens and the detector. The diameter of the condenser lens

$$a_c = 2\lambda F_o d_o.$$

Hence

$$a'_D = a_T \frac{2\lambda F_o}{a_c} \quad d'_o$$
$$= 2\lambda \Phi F_c^{\#}$$

where $F_c^{\#}$ is the F-number of the imaging cone of the condenser lens and Φ is the space bandwidth product.

The specific detectivity D* given by

$$D^* = \frac{\sqrt{\pi}}{2} a'_D (1/T_s)^{1/2} (S/N) \frac{D_F}{P_L T_o T_t} \quad (4)$$
$$= \sqrt{\pi} \; 2\lambda \Phi \; F_c^{\#} \sqrt{R} \sqrt{B} \; (S/N) \; \frac{D_F}{P_L T_o T_t}.$$

Hence the power required

$$P_L = \sqrt{\pi} \, 2\lambda\Phi \; F_c^{\#} \sqrt{R} \sqrt{B} \; (S/N) \; \frac{D_F}{T_o T_t} \; \frac{1}{D^*} \quad (5)$$

The ratio of laser powers required for both detector configurations:

$$\frac{P_{L2}}{P_{L1}} = \frac{\sqrt{2} \cdot F_c^{\#} \sqrt{R}}{X_D} \sqrt{\frac{B_2}{B_1}} \quad (6)$$

For the case when

$$\lambda = 6 \times 10^{-5} \text{cm}$$

$$\Phi = 1000$$

$$F_c^{\#} = 1$$

$$R = 32$$

$$X_D = 1.5 \text{ cms}$$

$$\frac{P_{L2}}{P_{L1}} = 1/3 \sqrt{\frac{B_2}{B_1}}$$

This ratio is not all that useful since the data rate for the second case is limited by mechanical rather than signal considerations. However, the above relationship shows that for a given power level, the second detector configuration permits greater dynamic range D_F to be accommodated.

Optical System Considerations

From an optical design point of view, the specification of the optical components used in an optical intensity spectrum measurement system are simple and can be adequately satisfied with "off the shelf" components. However, the design of the system configuration and the orientation of the components, stops and light baffles are important factors that determine the performance characteristics of the instrument. The analysis presented in this Section is usually ignored under the assumption that the effects are negligible. As is shown, however, under certain conditions demanded by unique applications, these effects can become significant.

Aberrations due to Film Substrate Tnickness

As stated earlier in this paper, the most desirable optical configuration for the optical intensity spectrum measurement system is to locate the transparency in the converging beam. For many mapping applications of OPS measurement in aerial photography, the input transparency is a 9" x 9" by 1/4" thickness plate. Also OPS systems in such applications involve some form of large aperture scanning systems incorporated with a regular OPS measurement configuration discussed earlier. One such configuration is illustrated in Figure 6 . In this Section the aberration contributions due to the thickness of the film substrate are considered.

When the scanning beam is on-axis the only aberration is spherical aberration. The lateral spherical aberration is given by (11)

$$\Delta h_s = \frac{(n^2-1)}{16n^3} - \frac{t}{(f_b^{\#})^3} \tag{7}$$

where n is the refractive index of the film substrate, t is its thickness and $f_b^{\#}$ is the F-number of the transforming optics defined by the scan aperture. Since the $f_b^{\#}$ is usually very large (20 or greater) it is clear that the spherical aberration is negligible compared to the diffraction limited spot size.

When the scanning beam is at the extreme converging angle, the film substrate is at an inclined angle to the beam. Hence, there is not only other off-axis aberrations such as coma and astigmatisms, but also there is a lateral displacement of the beam resulting in lateral displacement of the origin of the intensity spectrum. The astigmatic aberration is predominant and is given by (approximately for small scan angles) (11)

$$\Delta h_a = \frac{n^2-1}{16\,n^3} - \frac{t}{(f_T^{\#})^2 f_b^{\#}} \tag{8}$$

where $f_T^{\#}$ is the F-number of the transforming optics considering the entire scan format. Even under these conditions, it is clear that the aberrations are negligible compared to the diffraction limited spot size.

The lateral displacement of the scan beam is given by

$$\Delta h_d = \frac{(n-1)}{n} \quad \frac{t}{2 f_T^{\#}} . \tag{9}$$

For a typical case:

$n = 1.5$

$f_T^{\#} = 3$

$t = 6\text{mm}$

$\Delta h_d = 1/3\text{mm}.$

The displacement of the origin of the intensity spectrum by .3 mm is by no means negligible and could present serious problems.

Scan Center Stability and the Effect on Intensity Spectrum Stability

Consider the condition under which the scan center is longitudinally translated during scanning by Δf. Then the lateral displacement of the origin of the intensity spectrum can be shown to be

$$\Delta h_{sc} = \frac{\Delta f}{2 f_s f_s^{\#}} \cdot f_T \tag{10}$$

where f_s is the focal length of the telecentric scan forming optics, $f_s^{\#}$ is the F-number and f_T is the focal length of the transforming optics.

 6

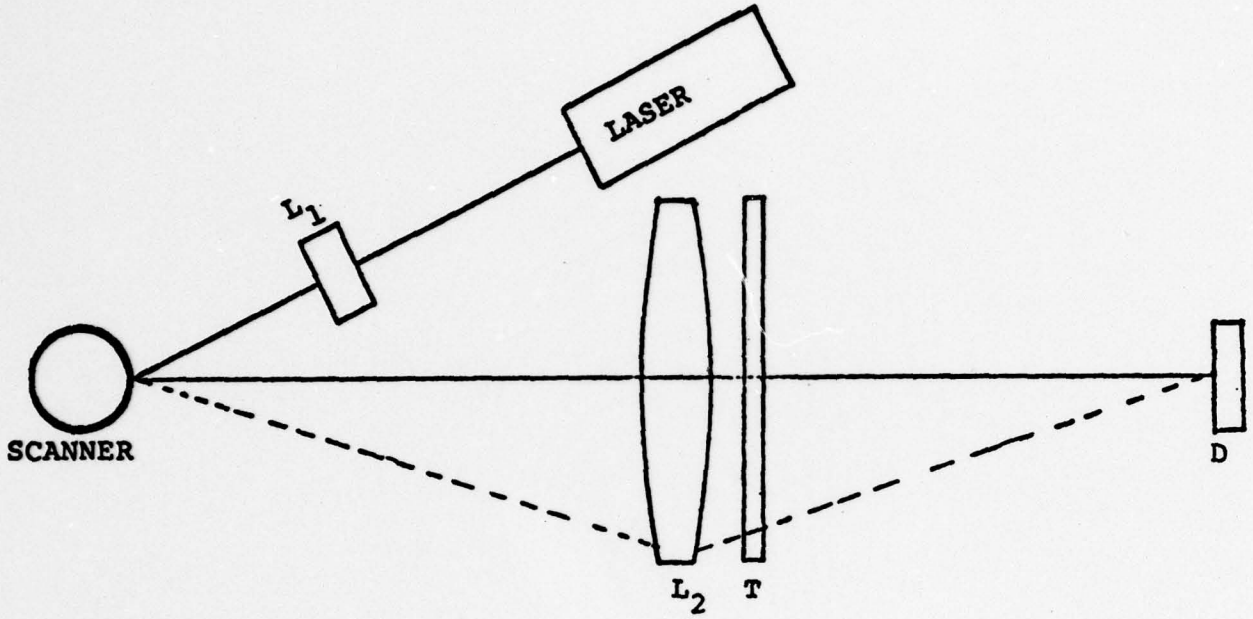

FIGURE A-6 OPS system with a beam scanner

Assume a multifaceted polygonal spinner is used to generate the scan pattern. For the scanner illustrated in Figure 7, the number of facets N is given by

$$N = 4\pi f_s^{\#}$$

The axial displacement of the scan center caused by the departure of the facets from a cylindrical surface is given by

$$\Delta f = \frac{\pi^2 D}{8N^2} = \frac{D}{128 (f_s^{\#})^2} \tag{11}$$

where D is the diameter of the scanning wheel. Substituting for Δf in equation (10)

$$\Delta h_{sc} = \frac{D}{256 (f_s^{\#})^3} \frac{f_T}{f_s} . \tag{12}$$

Consider the following example.

$$\frac{f_T}{f_s} = 1$$

$$D = 150 \text{ mm}$$

$$f_s^{\#} = 3 \qquad \text{Using equation (12)}$$

$$\Delta h_{sc} = 0.021 \text{ mm}$$

However if the scan forming optics focal length is doubled, $f_T/f_s = 1/2$ and $f_s^{\#} = 6$, then under these conditions

$$\Delta h_{sc} = 0.001 \text{ mm}$$

which is negligible. The parameters f_s and hence $f_s^{\#}$ can not be arbitrarily increased since not only does it drastically limit the smallest sampling aperture that can be obtained but also makes the overall system unduly large. Large optical lengths also tend to produce out of focus images of stops and aperatures placed in the back of the system at the intensity spectrum plane resulting in a large bias illumination. This can limit the dynamic range of the spectral distribution that can be measured.

The above considerations clearly demonstrate the need for careful analysis of the system configuration even though the individual components do not require any exhaustive design analysis.

Effects of Spatial and Temporal Coherence on OPS Measurement

In this section we briefly consider the effects of the spatial and temporal coherence of the incident wavefield upon the OPS measurement. For a monochromatic point source the intensity distribution in the transform plane is given by

$$I(f_x, f_y) = \left| T(f_x, f_y) * H(f_x, f_y) \right|^2 \tag{13}$$

where (f_x, f_y) represents spatial frequency, T is the transform of the transmission function, H is the transform of the sampling aperture function, and * represents a convolution operator. Since every detector has limited resolution, the measured output is expressed by

$$I(f_x, f_y) = \left| T(f_x, f_y) * H(f_x, f_y) \right|^2 * D(f_x, f_y) \tag{14}$$

where D is the detector sampling window expressed in terms of equivalent spatial frequency.

The effects of spatial coherence of the incident wavefield on the OPS measurement are easily seen if we consider the equivalent source distribution which gives rise to the wavefield. A wavefield with a given coherence can be viewed

W. Bala et al 7

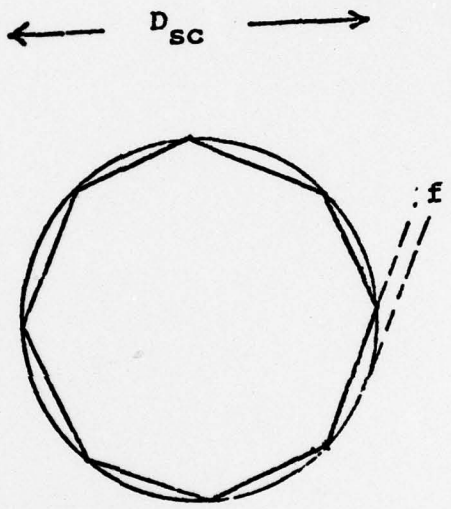

Figure A-7 Multifaceted Scanner

as arising from an extended array of incoherent monochromatic point sources whose intensity distribution is the fourier transform of the coherence function. Since the optical arrangement in Figure 1 images the source onto the transform plane, the resulting measurement is given by

$$I(f_x, f_y) = \left| T(f_x, f_y) * H(f_x, f_y) \right|^2 * D(f_x, f_y) * S(f_x, f_y) \quad (15)$$

where S represents the intensity image of the source scaled to spatial frequency coordinates.

The above equation shows the equivalence between effective source size (or equivalently wavefield coherence) and detector resolution. Both effects can be combined into an equivalent source size, or alternatively, an equivalent detector resolution. A consequence of this fact is the ability to simulate varying degrees of wavefield coherence by proper apodization of the detector sampling window.

The effects of temporal coherence are not as easily calculated as those of spatial coherence. If we consider the wavefield to consist of an ensemble of monochromatic components, then each component gives rise to an intensity distribution with a different scaling between distance in the transform plane and spatial frequency. These varying scale factors result in a "smeared" OPS distribution but the exact effects are more difficult to evaluate quantitatively. The variations in wavelength can also be viewed as a variation in d_o and hence can be related to equivalent errors in locating the transparency.

Summary

This paper has illustrated some of the practical design considerations required for implementation of an OPS measurment system. These considerations have necessarily been brief and were intended only to illustrate how the parameters associated with each of the system components can sometime significantly effect the system performance. The analysis has also shown that careful consideration be given to system configuration. The optimum configuration and the combination of parameters depends greatly on the intended application.

References

1. Lendaris, G. G., and G. L. Stanley, Diffraction Pattern Sampling for Automatic Pattern Recognition, Proc. IEEE, Vol. 58, pp. 128-216. 1970.
2. Jensen, N., High Speed Image Analysis Techniques, Photogrammetric Engineering, Vol. 39, pp. 1321-1328. 1973.
3. Lukes, G. E., Cloud Screening from Aerial Photography Applying Coherent Optical Pattern Recognition Techniques, Proc. SPIE, Coherent Optical in Mapping, Vol. 45, pp. 265-272. 1974.
4. Kasdan, H. L., Nonparametric Feature Analysis Methods for Sampled Diffraction Patterns, Proc. SPIE, Vol. 5. pp. 107-206. Oct., 1972.
5. Nill, N. B., Scene Power Spectra; The Moment as an Image Quality Merit Factor, Applied Optics, Vol. 15, page 2846. 1976.
6. Recording Optical Power Spectrum Analyzer, sold by Recognitions Systems Inc., Van Nuys, California.
7. Swantner, W., Lenses for Coherent Processing, Proc. IOCC Conf. 1976. IEEE Catalogue No. 76CH1100-7C.
8. Bieren, K. Von, Lens Design for Optical Fourier Transform Systems, Applied Optics, Vol. 10, page 2739. 1971.
9. Wynne, C. G., Simple Fourier Transform Lenses-II, Optics Communications, Vol. 12, page 270. 1974.
10. Goodman, J. W., Introduction to Fourier Optics, McGraw Hill, N. Y. 1968.
11. Smith, W., Modern Optical Engineering, McGraw Hill, N. Y. 1966.

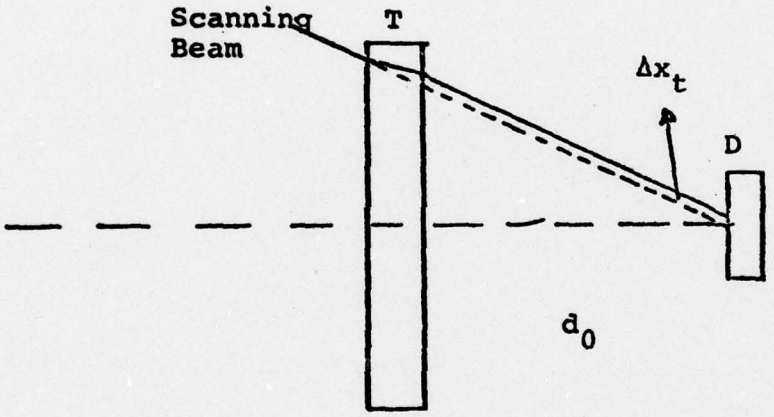

Figure A-8 OPS Translation due to Film Substrate Thickness